Geochemical Perspectives Letters

Refining Hf crust formation ages in Precambrian terranes

A. Petersson, T. Waight, A.I.S. Kemp, M.J. Whitehouse

Supplementary Information

The Supplementary Information includes:

Geological Setting

The Fennoscandian Shield preserves more than 3 Ga of crustal evolution and growth. It has an Archean nucleus, suggested to have its origin in the North Atlantic Craton (Petersson *et al.*, 2024a), in the northeast and increasingly younger Precambrian rocks towards the southwest, representing growth by progressive lateral accretion (Stephens, 2020). The Svecokarelian Orogen in central to northern Sweden and Finland is dominated by 3.2–2.6 Ga Archean basement and 2.5–2.0 Ga Paleoproterozoic cover rocks to the east of the Pajala deformation belt (Bergman *et al.*, 2006) and northeast of the Finnish Raahe–Ladoga shear complex (Kärki *et al.*, 1993). To the west and southwest of these respective shear zones, the dominant rocks formed between 1.9 and 1.8 Ga and are commonly agreed to have formed syn-orogenically during subduction-related processes in a convergent continental margin (*e.g.*, Hermansson *et al.*, 2008; Stephens, 2009; Petersson *et al.*, 2015a). Interestingly, southwest of the Pajala deformation belt, very little felsic magmatism has been recognised between *ca.* 2.5 and 2.1 Ga (*e.g.*, Claesson *et al.*, 1993; Bingen and Solli, 2009). Post *ca.* 2.1 Ga, the Fennoscandian Shield entered a stage of continental growth *via* lateral accretion of microcontinents and volcanic and continental arcs that ended in a continental collision (Korja *et al.*, 2006). Magmatic activity began at *ca.* 2.02 Ga, peak activity has been recorded to between 1.91 and 1.87 Ga, and between 1.82 and 1.75 Ga post-collisional granitic magmatism took place (Bingen and Solli, 2009). This Svecokarelian magmatic event was accompanied by metamorphism and reworking of existing crust (*e.g.*, Bergman *et al.*, 2001; Weihed *et al.*, 2005). Subsequently, the mainly felsic alkali-calcic magmatism of the N-S trending Transscandinavian Igneous Belt was emplaced episodically between *ca.* 1.89 and 1.65 Ga (*e.g.*, Högdahl *et al.*, 2004). Within the Eastern Segment of the Sveconorwegian Orogen, a parautochthonous domain comprising reworked rocks of the Transscandinavian Igneous Belt is made up of predominantly felsic rocks ranging from *ca.* 1.86 to 1.60 Ga, with increased magmatic activity between *ca.* 1.80 and 1.64 Ga. This activity peaks at 1.80, 1.69 and 1.68 Ga (Appelquist *et al.*, 2008; Bingen *et al.*, 2008; Connelly *et al.*, 1996; Rimša *et al.*, 2007; Söderlund *et al.*, 1999, 2002, 2008). This basement was subsequently intruded by rapakivi granite plutons at *ca.* 1.65–1.50 Ga (Haapala *et al.*, 2005). The next major orogenic events to

affect the Fennoscandian Shield were the *ca.* 1.47–1.41 Ga Hallandian (Eastern Segmant; Hubbard, 1975; Brander and Söderlund, 2009) and Danopolonian (East and South of the Protogene Zone; Bogdanova *et al.*, 2008; Waight *et al.*, 2012; Johansson *et al.*, 2016) orogenies.

Central and northern Sweden can be divided into different lithotectonic units, with the Norrbotten unit in the north, the Överkalix unit in the northeast and the largest unit, the Bothnia-Skellefteå unit, covering a large area from north of the Hagsta Gneiss Zone to just south of Luleå and Jokkmokk (Stephens and Bergman, 2020). The two northernmost units, the Norrbotten and Överkalix lithotectonic units are unique in that they are the only units that host Archean rocks (*ca.* 2.8–2.6 Ga). However, Archean rocks only crop out in the southernmost part of the Överkalix unit (the Simo Complex) and in the northernmost parts of the Norbotten unit (the Råstojaure Complex), and hence our understanding of the earliest evolution of north-western Fennoscandia is limited to these scarce outcrops (Bergman and Weihed, 2020). During accretionary growth towards the present day southwest, Paleoproterozoic mafic and ultramafic rocks intruded the Archean basement between 2.5 and 2.4 Ga and together were overlain by syn-orogenic *ca.* 2.0–1.8 Ga supracrustal rocks (Gaál and Gorbatschev, 1987). Between *ca.* 1.9 and 1.8 Ga, mainly felsic volcanic rocks were emplaced during a period of accretionary tectonics along an active continental margin (Bergman and Weihed, 2020). Turbiditic greywacke and argillite deposited between *ca.* 1.96 Ga and 1.86 Ga dominate the Bothnian basin (in the Bothnia-Skellefteå unit), and were intruded by sequential magmatic pulses at 1.95–1.93, 1.90–1.88, 1.87–1.85 and 1.81–1.76 Ga (Skyttä *et al.*, 2020). Metamorphic grade and deformation vary and are connected to the major shear zones in the region (Skyttä *et al.*, 2020).

Analytical Protocol

Zircon U-Pb SIMS age determination

SIMS (Secondary ion mass spectrometry) U-Pb isotope analyses, and age determination of zircon were carried out using a large geometry CAMECA IMS1280 at the Swedish Museum of Natural History in Stockholm, Sweden. Instrument set-up closely followed that of Whitehouse *et al.* (1999) and Whitehouse and Kamber (2005). An O_2^- primary beam with −13 kV primary and +10 kV secondary was used during sputtering. The primary beam operated using a hyperion source in critical focusing mode, and a 5 µm raster, resulting in *ca.* 15 µm spots. Automatic pre-sputtering using a 25 µm raster for 120 s; centring of the secondary ion beam in the 3000 µm field aperture (FA), mass calibration optimization, and optimization of the secondary beam energy distribution were executed for each run. FA and energy adjustment were optimized using the $^{90}Zr_2{}^{16}O^+$ species at nominal mass 196. At the start of each session, mass calibration of all peaks in the mono-collection sequence was done; within-run mass calibration optimization was performed using the $^{90}Zr_2{}^{16}O^+$ peak, applying a shift to all other species. A mass resolution (M/ΔM) of *ca.* 5400 was used to guarantee satisfactory separation of Pb isotope peaks from nearby HfSi+ masses. Ion-signals were detected using an axial ion-counting electron-multiplier. Analyses were run in fully automated sequences. The data reduction assumes a power-law relationship between Pb^+/U^+ and UO_2^+/U^+ with an empirically derived slope used to calculate actual Pb/U, which are based on results from the reference zircon 91500. Concentration of U and the Th/U are referenced to the M257 zircon standard. Common Pb correction was made in cases where the ^{204}Pb signal exceeded average background and was assumed to have a $^{207}Pb/^{206}Pb$ ratio of 0.83 (equivalent to present day model terrestrial Pb; Stacey and Kramers, 1975). Decay constants follow the recommendations of Jaffey *et al.* (1971) compiled by Steiger and Jäger (1977). All age calculations were done using Isoplot 4.15 (Ludwig, 2008) and are quoted at the 2σ uncertainty level. External uncertainties in standard zircon analyses are propagated. All data from secondary reference zircon, 91500 and OGC, yield results that are within uncertainties indistinguishable from their respective accepted reference values. All zircon U-Pb results are presented in Table S-1.

Ion microprobe oxygen isotope analysis in zircon

Zircon oxygen isotopes ($^{18}O/^{16}O$) were analysed using the same large geometry CAMECA IMS1280 at the Swedish Museum of Natural History in Stockholm, Sweden. Post U-Pb analyses, the sample mounts were carefully cleaned using detergent, distilled water followed by submerging the sample in ethanol in an ultrasonic bath. The samples were subsequently recoated with a 30 nm coat of Au. Pre-sputtered was carried out over a 10 × 10 µm area with a 10 kV, Gaussian Cs^+ beam and an intensity of *ca.* 2–3 nA yielding a total impact energy of 20 keV. To ensure charge compensation during the analyses, an electron gun was used. Secondary ions were admitted into the double focusing mass spectrometer *via* a 170 µm entrance slit and then focused in the centre of a 2500 µm field-aperture (FA) (×100

magnification). The ions were energy filtered using a 30 eV band pass with a 5 eV gap toward the high-energy side. ^{16}O and ^{18}O were simultaneously collected using Faraday cup detectors fitted with 10^{10} Ω (L'2) and 10^{11} Ω (H1) resistors, respectively, working at a mass resolution M/ΔM ≈ 2500. The magnetic field was controlled using nuclear magnetic resonance (NMR) control. All analysis involved a 30 s pre-sputtering to remove the Au-coating, which was followed by an automatic centring of the secondary ions in the field aperture (FA), in the contrast aperture and the entrance slit. All analyses subsequently comprised of twelve four-second cycles, yielding an average internal precision of *ca.* 0.1 ‰ (2 s.d.). At least two bracketing standards between every five to six unknown (sample) analyses were used to monitor the analytical session for drift. Instrumental mass fractionation (IMF) was corrected for using the standard reference zircon 91500 (Wiedenbeck *et al.*, 2004). Spot to spot reproducibility was 0.29 ‰ during session 1 and 0.31 ‰ during session 2 (2 s.d.) on 91500 zircon standards. Additional zircon references, M257 (Nasdala *et al.*, 2008) and OGC (Petersson *et al.*, 2019a), were used for quality control. The $\delta^{18}O$ uncertainty for each analysis was calculated by propagating the uncertainty of the IMS determination, including the standard deviation (s.d.) of the average $^{18}O/^{16}O$ measured on the primary standard (91500) during each session and the internal uncertainty on each analysis. Raw $^{18}O/^{16}O$ and corrected $\delta^{18}O$, including data for all reference zircon analyses (all quoted with respect to Vienna Standard Mean Ocean Water, VSMOW) are presented in Table S-2.

LA-MC-ICP-MS zircon Lu-Hf analyses

Zircon Lu-Hf analyses were performed using a 193 nm Cetac Analyte G2 excimer laser, a two-volume HelEx2 sample cell, and a Thermo-Scientific Neptune+ multicollector ICP-MS, at the School of Earth Sciences at the University of Western Australia. The spot of the Lu-Hf analyses overlapped pits from the SIMS U-Pb analyses, and wherever possible, also the O isotope analyses. Circular laser spots were used, with a diameter of 40–50 µm. A 60 s baseline measurement preceded all analysis, and was by followed by an ablation sequence of 60 s, comprising 60 integration cycles of one second each. A 4 Hz laser pulse repetition rate was used and a laser energy of *ca.* 5 J/cm^2. That equals an ablation rate of approximately 0.05 µm per pulse for zircon. A He-carrier gas, set to 1.0 L/min, was used to carry the ablated particles from the sample chamber to the plasma. The He gas was combined with Ar-gas, using a flow rate of *ca.* 0.6 L/min and N gas (*ca.* 0.012 L/min) further downstream prior to entering the argon plasma. Masses ^{171}Yb, ^{173}Yb, ^{175}Lu, ^{176}(Hf+Lu+Yb), ^{177}Hf, ^{178}Hf, ^{179}Hf and ^{180}(Hf+W+Ta) were measured simultaneously using Faraday cups. Isobaric interference of ^{176}Yb and ^{176}Lu on ^{176}Hf was calculated using the measured intensities of ^{171}Yb and ^{175}Lu along with the known ratios of $^{176}Lu/^{175}Lu = 0.02655$ (Vervoort *et al.*, 2004) and $^{176}Yb/^{171}Yb = 0.897145$ (Segal *et al.*, 2003). The exponential law was used to calculate the mass bias corrections. The measured intensities of ^{179}Hf and ^{177}Hf and a $^{179}Hf/^{177}Hf$ ratio of 0.7325 were used for calculations of βHf, and βYb was calculated using the measured intensities of ^{173}Yb and ^{171}Yb and the known ratio of $^{176}Yb/^{171}Yb = 1.130172$ (Segal *et al.*, 2003). The mass bias behaviour of Lu was assumed identical to that of Yb. Mud Tank was used as the primary zircon reference, and three secondary zircon standards (FC1, R33 and OGC) were used for quality control. All standard results correspond with accepted reference values. FC1: weighted mean $^{176}Hf/^{177}Hf = 0.282188 \pm 0.000003$ ($n = 31$, 2σ, solution reference $^{176}Hf/^{177}Hf = 0.282184 \pm 0.000016$; Woodhead and Hergt, 2005); R33: weighted mean $^{176}Hf/^{177}Hf = 0.282760 \pm 0.000005$ ($n = 16$, 2σ, solution reference $^{176}Hf/^{177}Hf = 0.282764 \pm 0.000014$; Fisher *et al.*, 2014); OGC: weighted mean $^{176}Hf/^{177}Hf = 0.280640 \pm 0.000004$ ($n = 17$, 2σ, reference $^{176}Hf/^{177}Hf = 0.280633 \pm 0.000034$; Kemp *et al.*, 2017). The analysed $^{176}Hf/^{177}Hf$ of the unknown sample zircon were normalised based on a comparison between the average of analysed $^{176}Hf/^{177}Hf$ of the Mud Tank reference zircon measured in the given session and its known $^{176}Hf/^{177}Hf = 0.282507$ determined *via* solution analysis (Woodhead and Hergt, 2005) and itself reported relative to the JMC475 $^{176}Hf/^{177}Hf = 0.282160$. Zircon Lu-Hf isotope data are summarised in Table S-3.

Two-stage Hf model ages have been calculated using the $^{176}Lu/^{177}Hf$ of the zircon for the first step (back-calculating to the age of zircon crystallisation), and an interpreted source $^{176}Lu/^{177}Hf$ for the second step (from crystallisation – back to mantle differentiation of the source material). $^{176}Lu/^{177}Hf = 0.009$ for a felsic source, $^{176}Lu/^{177}Hf = 0.0115$ for a bulk continental source and $^{176}Lu/^{177}Hf = 0.022$ for a mafic source (Vervoort and Patchett, 1996; Rudnick and Gao, 2003).

Zircon BSE images and all spot locations of all analyses are found on Figures S-1 and S-2.

Figure S-1 Zircon BSE images and spot locations for U-Pb, O and Lu-Hf isotope analyses.

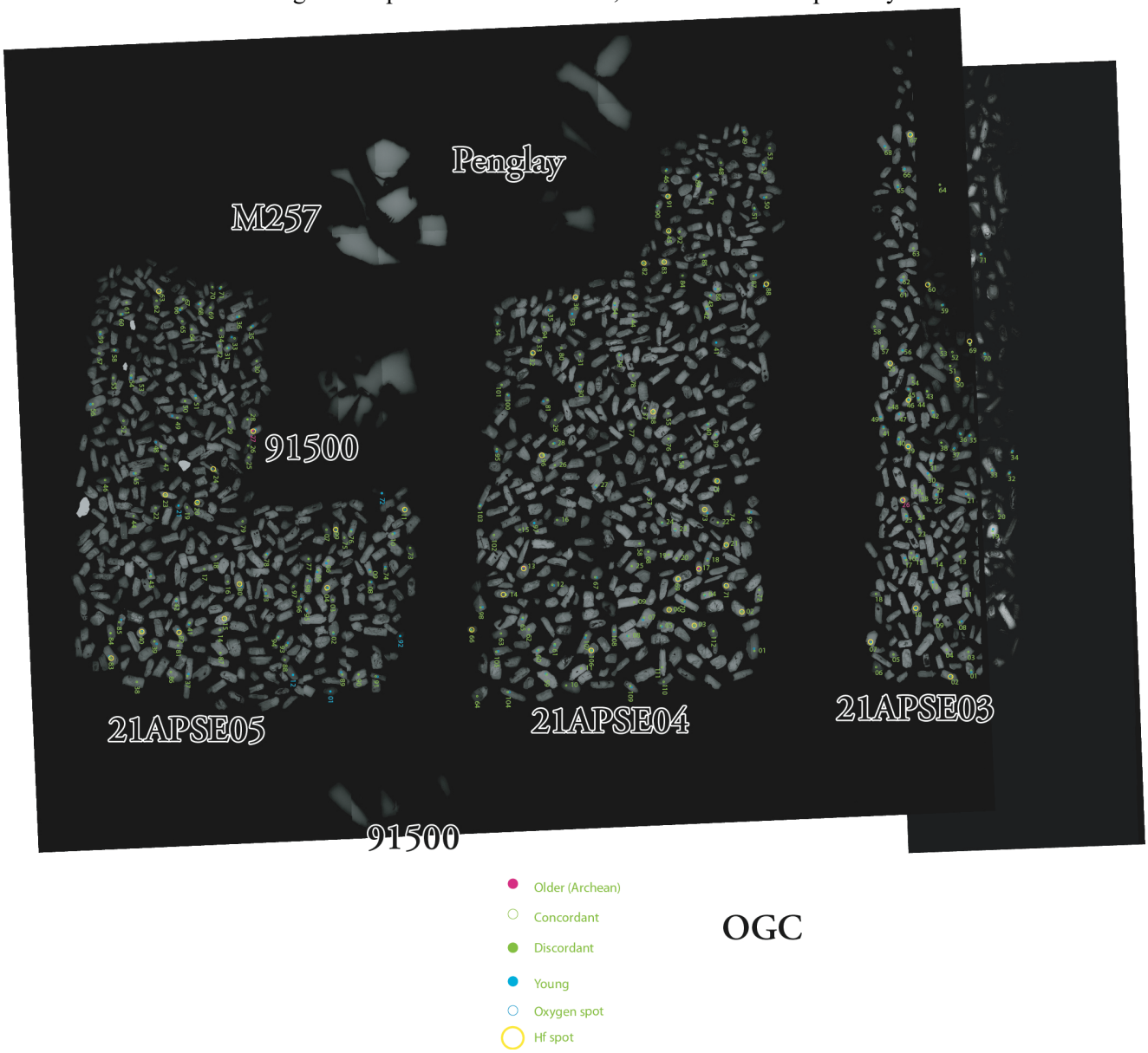

Figure S-2 Zircon BSE images and spot locations for U-Pb, O and Lu-Hf isotope analyses.

Samples and Results

Zircon Data Filtering

To ensure data quality, and to minimise possible effects of Pb-loss, and erroneous ages, a strict cut-off of 1 % discordance at the 2σ-level (at closest approach to the ellipse) has been implemented. Additionally, all individual analysis with uncertainties in excess of 25 Ma for the $^{207}Pb/^{206}Pb$ date (at the 1σ-level), which are largely the result of high common Pb corrections, are also omitted from further consideration.

21APSE04 Luleå River

The sample locality is within the Norrbotten lithotectonic unit that predominantly consists of 1.91–1.87 Ga granites and syenites, but rare occurrences of Archean *ca.* 2700–2650 Ma TTG occur (Lundqvist *et al.*, 1996, 2000; Öhlander and Schöberg, 1991). The actual sampling site is underlain by 1891 ± 32 Ma metagranodiorite (Mellqvist *et al.*, 2003), but less than 20 km upstream a granodioritic gneiss was dated to 2661 ± 3 Ma (Sadeghi and Hellström, 2018) and across the river from the sampling locality, a granite xenolith in the Bälinge magmatic breccia was dated to 2638 ± 19 Ma (Wikström, 1996).

Among the *ca.* 400 picked grains, the majority are subhedral with rounded external features and very few grains have sharp pyramidal terminations. The zircons vary between 50 and 400 μm in length along their C-axis. The zircons vary from clear to dark yellow and brown and some are cracked. Rounded grains are commonly more cracked and are darker coloured. Complex grains with visible cores and rims make up about 50 % of the sample population, and the majority of all grains show igneous oscillatory zoning in BSE, but clear and unzoned grains also occur.

Zircon Isotope Data

U-Pb analyses in 111 grains, of which 101 remain after data filtering, give $^{207}Pb/^{206}Pb$ dates between 2693 Ma and 1350 Ma. A majority of the analyses (n = 95), however, yield dates between 1937 Ma and 1776 M, with only two analyses, n6476-13 and n6476-17, recording Archean dates. Three grains give $^{207}Pb/^{206}Pb$ dates around 1600 Ma, one at 1350 Ma. Two main clusters of dates form peaks at *ca.* 1800 Ma and *ca.* 1880 Ma. Th/U range between 0.1 and 1.3 with an average of 0.4, and there is a general decrease in Th/U with decreasing age.

Seventy spots, all in different concordant zircon grains were analysed for O-isotopes, returning ratios equivalent to $\delta^{18}O$ ranging between 4.7 ‰ and 8.0 ‰. Eleven analyses yield signatures within uncertainty of mantle values (5.3 ‰ ± 0.6, 2σ; Valley *et al.*, 2005), while the remaining 63 analyses give heavier signatures.

Hf isotopes analyses of twenty-one dated zircon (2693 Ma to 1638 Ma) yield measured $^{176}Hf/^{177}Hf$ ranging between 0.28102 and 0.28186. Corresponding $\varepsilon_{Hf(t)}$ range from −3.9 to +4.2. No obvious trends can be deciphered in the Proterozoic zircon, and the Archean zircon (n = 2) gives $\varepsilon_{Hf(t)}$ of −2.7 and + 1.1 respectively.

21APSE05 Skellefteå River

Rocks in the surroundings of the sample locality are dominated by 1.91 to 1.87 Ga granites and subordinate syenites belonging to the Bothnia-Skellefteå lithotectonic unit (Rutland *et al.*, 2001; Weihed *et al.*, 2002; Guitreau *et al.*, 2014). The closest dated rock is, however, a 1798 ± 4 Ma granite (Weihed *et al.*, 2002), but upstream the majority of the dated intrusions fall within the 1.91 to 1.87 Ga age span (*e.g.*, González-Roldán, 2010; Bejgarn *et al.*, 2013; Mercier-Langevin *et al.*, 2013).

In this sample *ca.* 300 grains have overall euhedral to subhedral external morphologies with about 50 % of the grains having clearly rounded features and *ca.* 10 % have sharp pyramidal terminations. In size this zircon population vary between 50 and 350 μm along their C-axis. The colours vary from clear to dark yellow and brown and some with cracks. Rounded grains are commonly more cracked and are darker coloured. Complex grains with visible cores and rims make up about 50 % of the sample population, and the majority of all grains show igneous oscillatory zoning in BSE, but clear and unzoned grains also occur.

Zircon Isotope Data

Ninety-nine U-Pb analyses, of which eleven were discarded due to above stated criteria, give $^{207}Pb/^{206}Pb$ dates between 2694 Ma and 930 Ma. The majority of the analyses (n = 72) give dates between 1938 Ma and 1780 Ma, with a single Archean (2694 Ma) grain and 15 analyses giving dates younger than 1780 Ma. Two main clusters of dates

form peaks at *ca.* 1800 Ma and *ca.* 1900 Ma. Th/U range between 0.01 and 1.0 with an average of 0.4, with no correlation between Th/U and age.

Fifty-one O-isotope analyses, of which one (−68) was omitted due to analysing a crack, yield $\delta^{18}O$ ranging between 5.0 ‰ and 9.2 ‰. Six analysed grains yield signatures within uncertainty of mantle values.

Thirteen dated 2694 Ma to 1797 Ma zircons were analysed for Lu-Hf isotopes and yield $^{176}Hf/^{177}Hf$ ranging between 0.28111 and 0.28189. Corresponding $\varepsilon_{Hf(t)}$ ranges from +1.0 to +7.6. Zircons with *ca.* 1800 Ma dates yield $\varepsilon_{Hf(t)}$ between +1.0 and +4.7, while zircons aged between 1910 Ma and 1850 Ma yield the most radiogenic signatures with $\varepsilon_{Hf(t)}$ between +5.4 and +7.6. The 2694 Ma zircon gives a $\varepsilon_{Hf(t)}$ of +1.2.

21APSE03 Umeå River

Few rocks have been dated close to the sampling locality, but the general region of the Svecofennian Bothnian Basin around Umeå is dominated by *ca.* 1.95–1.85 Ma plutonic rocks (Lundqvist *et al.*, 1998). Upstream, in the Knaften region 1954–1939 Ma granites (Wasström, 1993; Wasström *et al.*, 2019) and 1866 ± 11 Ma dioritic intrusions (Billström *et al.*, 2002) have been dated. Further upstream two granodiorites have been dated to 1890 ± 7 Ma (Welin *et al.*, 1993) and 1902 ± 2 Ma (Björk and Kero, 1996).

Among the *ca.* 300 picked grains, the majority are euhedral to subhedral with about 50 % of the grains having rounded external features and *ca.* 10 % have sharp pyramidal terminations. In size the grains vary between 50 and 300 µm in length along their C-axis. The zircon morphology and colour vary vastly from clear homogeneous to dark yellow and brown and some grains are cracked. Complex grains with visible cores and rims make up about 25 % of the sample population, and the majority of all grains show igneous oscillatory zoning in BSE.

Zircon Isotope Data

Seventy-one analyses, all in different grains, of which four were omitted, yield $^{207}Pb/^{206}Pb$ dates between 2350 and 935 Ma. The vast majority of the data (*ca.* 80 %) cluster around 1800 Ma, with *ca.* 10 % of the analyses yielding dates between 1943 Ma and 1896. One concordant grain gives a $^{207}Pb/^{206}Pb$ date of 2350 Ma and four analyses return dates between 1249 and 935 Ma. Th/U ranges from 0.01 to 1.0 but most analyses have ratios close to the mean of 0.42, and there is no correlation between date and Th/U. The two main age groups do not differ morphologically, but the oldest grain, n6411-26, is rounded and unzoned in BSE. The main age-cluster forms a peak at *ca.* 1805 Ma with smaller peaks at *ca.* 1905 Ma (n = 5) and ca 1940 Ma (n = 2).

Forty-five analyses, all in different concordant zircon grains yield $\delta^{18}O$ ranging between 6.0 ‰ and 9.6 ‰, with only one grain (−10) within uncertainty of the mantle reference values.

Eleven dated 2350 Ma to 1801 Ma zircon were analysed for Lu-Hf isotopes and yield $^{176}Hf/^{177}Hf$ ranging between 0.28114 and 0.28182. Corresponding $\varepsilon_{Hf(t)}$ range between −5.4 and +8.2. While the *ca.* 1800 Ma zircons cluster around chondritic signatures, two 1935 and 1911 Ma zircons give the most radiogenic signatures in this study, with $\varepsilon_{Hf(t)}$ of +8.2 and +8.0. The oldest zircon grain in this river population gives a $\varepsilon_{Hf(2350\ Ma)}$ of −5.4.

21APSE06 Ångerman River

Rocks surrounding the sampling locality are from the Bothnia-Skellefteå lithotectonic unit and are dominated by 1.85–1.75 Ga granitic rocks, as well as Proterozoic (post-1.8 Ga) magmatic and sedimentary rocks. The most proximal dated rocks upstream include the 1931 ± 11 Ma Seltjärn granodiorite (Claesson and Lundqvist, 1995; Lundqvist *et al.* 1998); a pegmatite, dated using U-Pb on columbite-tantalite to 1795 ± 1 Ma (Romer and Smeds, 1997) and a 1870 ± 2 Ma metarhyolite (Lundqvist *et al.*, 1998).

Of the *ca.* 300 picked grains about 50 % are clear grains with sharp terminations. The remaining zircon grains vary from clear to dark brown with slightly rounded features. Zircon size vary between *ca.* 50 and 400 µm along their C-axis. Oscillatory zonation is the most common feature seen in BSE, but patchy irregular zonation is also common. Complex grains with cores and rims make up *ca.* 25 % of the populations.

Zircon Isotope Data

Eighty-six U-Pb analyses in 85 different grains, of which 14 were discarded due to discordance and two due to excessive uncertainties, yield $^{207}Pb/^{206}Pb$ dates between 2062 Ma and 986 Ma. The majority of the data (n = 67) give dates ranging between 1883 Ma and 1783 Ma with a major peak at *ca.* 1800 Ma and a minor peak at *ca.* 1870 Ma. One

grain gives an older date at 2062 Ma and two grains yield <1300 Ma dates. Th/U ranges between 0.8 and 0.2 with a mean of 0.3 and there is no correlation between Th/U and dates.

Of thirty-six analyses, all in different concordant grains, one (−48) was omitted due to analysing an inclusion. The remaining 35 analyses return signatures that correspond to zircon $\delta^{18}O$ ranging between 8.1 ‰ and 9.7 ‰.

Thirteen dated 2168 Ma to 1802 Ma zircons were analysed for Lu-Hf isotopes and yield $^{176}Hf/^{177}Hf$ ranging between 0.28117 and 0.28169. Corresponding $\varepsilon_{Hf(t)}$ ranges between −9.1 and +1.9. The *ca.* 1800 Ma zircons cluster at slightly supra-chondritic signatures (+0.4 to +1.1), while 1880–1870 Ma zircons give slightly sub-chondritic signatures (−0.1 to −1.3). The oldest grain in this sample, a 2168 Ma grain yields a strongly negative $\varepsilon_{Hf(t)}$ of −9.1.

21APSE07 Indal River

The sample locality is within the Bothnia-Skellefteå unit and the principal surrounding geology is dominated by 1.85–1.75 Ga granitic rocks and metagreywacke, mica schist, graphite- and/or sulphide-bearing schist, paragneiss, migmatite, quartzite, amphibolite (*ca.* 1.96–1.87 Ga). The closest dated igneous rocks are the 1863 ± 6 Ma Härnö Granite (Högdahl *et al.*, 2012) and the 1891 ± 12 Ma Helvetesbrännan granodiorite (Delin and Aaro, 2002). Upstream a quartzite has been dated to an upper intercept age of 1993 ± 4 Ma using discordant detrital zircon (Welin *et al.*, 1993) and a granodiorite to 1883 ± 14 Ma (Lundqvist and Lundin, 1999).

About 300 grains were picked from this sample, which consists of *ca.* 50 % clear and 50 % brown (turbid) crystals that range in size from 50 to 350 µm along their C-axis. Grains are commonly slightly rounded to subhedral, but euhedral grains are present with a higher proportion amongst the clear grains. Oscillatory zoning is most common in BSE, but unzoned and sector zoned grains occur. Grains with cores and rims are common, especially amongst larger brown grains.

Zircon Isotope Data

Eighty-four analyses, of which six were discarded due to >1 % discordance at the 2σ level, have a range in $^{207}Pb/^{206}Pb$ dates if between 3115 Ma and 1025 Ma. The data form two main age peaks at *ca.* 1800 Ma (n = 24) and *ca.* 1870 Ma (n = 19), and a smaller peak at *ca.* 1980 Ma (n = 6). Four >99 % concordant analyses yield Archean dates, and one 1.6 % discordant analysis gives a date of 3257 Ma. Three analyses give < 1600 Ma dates. Th/U ranges between 1.2 and 0.05 with an average of 0.4 with a slight correlation between Th/U and dates, where the most extreme Th/U are found in grains within the 1979–1780 Ma range.

Fifty-eight different zircon grains were analysed for O-isotopes, of which four (−10, −44, −47 and −72) were discarded due to analysing a crack and/or inclusion. Of the remaining 54 analyses, two analysed zircons yield signatures within uncertainty of the depleted mantle reference, and the remainder spread to heavier values ($\delta^{18}O$ ranging between 5.4 ‰ and 10.7 ‰). The 3257 Ma grain from the Indal river gives a $\delta^{18}O$ of +7.8, but since the U-Pb is slightly (1.6 %) discordant, and hence shows indication of disturbance, this result may be unreliable.

Twelve Hf isotope analyses of zircon grains dated to 3115–1861 Ma return $^{176}Hf/^{177}Hf$ ranging between 0.28094 and 0.28160. Corresponding $\varepsilon_{Hf(t)}$ range between −2.2 and +3.9. The two *ca.* 1870 Ma grains give slightly sub-chondritic signatures, while five 1997–1968 Ma zircons cluster just above chondritic values. The oldest 3115 Ma grain in this sample yields the most radiogenic signature with an $\varepsilon_{Hf(t)}$ of +3.9. One more zircon (−43), a 3257 Ma grain, was analysed, but as the grain was too small for the 40 µm beam to sample purely core, and the analyses yield a mixed signal of core and rim (of unknown age) returning a Hf isotope signature corresponding to a $\varepsilon_{Hf(t)}$ of +22, clearly erroneous. This analysis was hence omitted from further considerations. Due to the small size of the zircon grain and core (<40 µm wide), a similar scenario with less incorporation of rim, is likely for the 3115 Ma grain (−44) analysis. Hence, the $\varepsilon_{Hf(3115\ Ma)}$ of +3.9 is considered unreliable, and this analysis is omitted from further considerations.

21APSE08 Ljungan River

The area immediately up stream belongs to the Bothnia-Skellefteå unit. The predominant lithologies in the surrounding area is made up of granite, pegmatite, granodiorite and subordinate diorite and gabbro (*ca.* 1.87–1.84 Ga) as well as metagreywacke, mica schist, graphite- and/or sulphide-bearing schist, paragneiss, migmatite, quartzite, amphibolite (*ca.* 1.96–1.87 Ga) (Högdahl *et al.*, 2012). The closest dated igneous rocks, *ca.* 3 km to the northeast, are the Härnö granite, 1863 ± 6 Ma (igneous monazite age from Högdahl *et al.*, 2012). Further upstream, close to the

border to the Ljusdal lithotectonic unit, Delin and Aaro (1994) dated a metagranite to 1856 ± 19 Ma, and Wilson *et al.* (1985) dated the Rätan granite to 1698 ± 25 Ma, both using ID-TIMS on zircon.

Of the *ca.* 400 picked grains the majority are brownish, cracked and rounded of which many have clear cores and rims. Clear, more euhedral zircon occur, but in lesser amounts compared to the other samples in this study. The size range is similar, 50 to 4000 µm along their C-axis, but the average size is larger than in the other samples. BSE imaging reveals many grains with complex zonation patterns and core/rim relations, but overall oscillatory zonation is the most common feature.

Zircon Isotope Data

Seventy-five analyses, of which six were discarded due to >1 % discordance at the 2σ level and one due to excess uncertainties, yield $^{207}Pb/^{206}Pb$ dates between 2742 Ma and 1499 Ma. The majority of the data form a peak at *ca.* 1865 Ma with a smaller peak at *ca.* 1930 Ma. Ten grains give dates between 2035 Ma and 1959 Ma and a group of five analyses form a concordant cluster at *ca.* 2725 Ma. Th/U ranges between 1.4 and 0.0 with no correlation apparent between dates and Th/U.

Out of 57 zircon O-isotope analyses all but one (−18, 0.5 % disc.) in concordant grains, two analyses (−29 and −53) were omitted due to analysing a crack and/or inclusion. The remaining 55 analyses return $\delta^{18}O$ ranging between 5.2 ‰ and 10.3 ‰. Eight analyses are within uncertainty of the mantle reference values.

Sixteen zircon Hf isotope analyses of dated 2742–1551 Ma grains return $^{176}Hf/^{177}Hf$ ranging between 0.28103 and 0.28179, corresponding to a range in $\varepsilon_{Hf(t)}$ between −3.5 and +6.1. The two *ca.* 1870 Ma grains give slightly sub-chondritic signatures, while five 1997–1968 Ma zircons cluster just above chondritic. The Proterozoic (2035–1855 Ma) zircon spread between −3.5 and +4.9, while the Archean (2742–2680 Ma) zircon give $\varepsilon_{Hf(t)}$ between −1.4 and +3.5.

Supplementary Discussion

Ensuring primary signatures

Th/U of the analysed zircons from all samples ranges from 0.01 to 1.43 with an average of 0.47, where 76 % of the analyses yield Th/U > 0.3 suggesting primarily magmatic signatures (Fig. S-3). Low (<0.3) Th/U zircon are exclusively restricted to the period around the Svecokarelian Orogeny (2.0–1.8 Ga), but as there is no correlation between Th/U and $\varepsilon_{Hf(t)}$, nor between Th/U and $\delta^{18}O$. Fifteen analyses, with the majority from the Indal and Ljungan rivers, yield Th/U < 0.1, and hence a metamorphic origin for these rocks can't be dismissed entirely. However, as no other data from these grains ($^{207}Pb/^{206}Pb$, $\delta^{18}O$, $\varepsilon_{Hf(t)}$) deviate from remaining populations metamorphic effects on these isotopic ratios are deemed negligible (Fig. S-3).

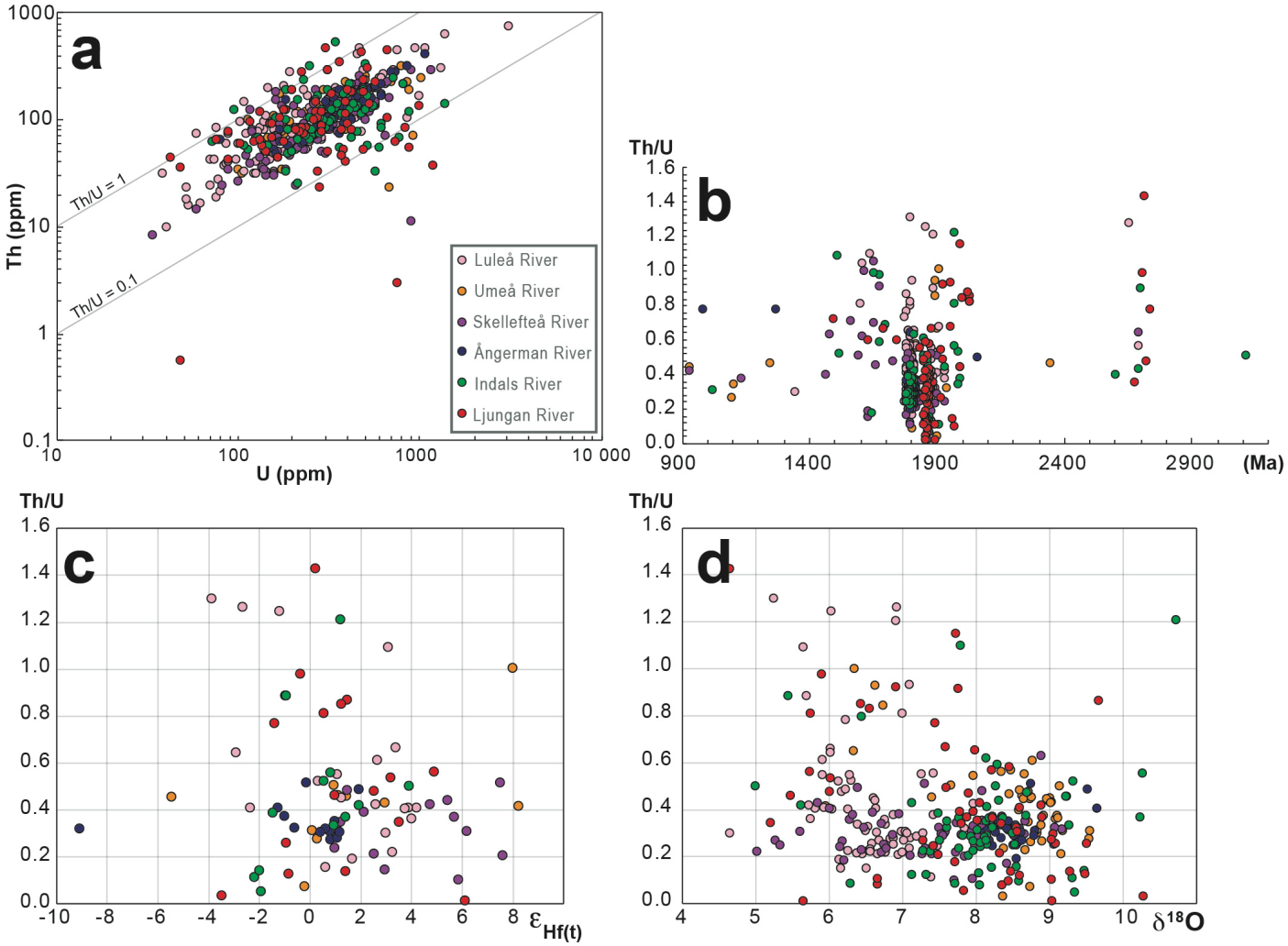

Figure S-3 **(a)** Zircon Th (ppm) *versus* U (ppm). **(b)** Zircon Th/U *versus* $^{207}Pb/^{206}Pb$ dates (Ma). **(c)** Zircon Th/U *versus* $\varepsilon_{Hf(t)}$. **(d)** Zircon Th/U *versus* $\delta^{18}O$.

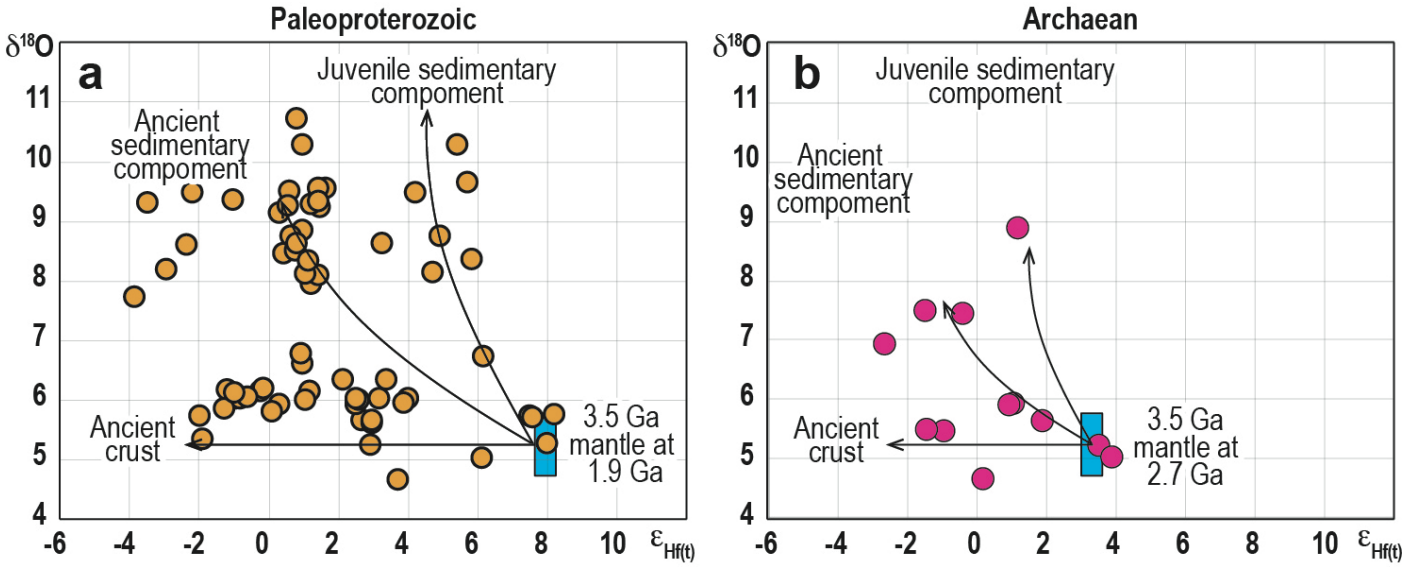

Figure S-4 Zircon $\delta^{18}O$ *versus* zircon $\varepsilon_{Hf(t)}$ showing isotopic trends tracing back to a *ca.* 3.5 Ga chondritic mantle. Blue boxes denote mantle composition at 1.9 Ga and 2.7 Ga respectively. **(a)** <2.0 Ga zircons. **(b)** Archean zircons.

Literature data filtering

Very few data-points plot above the regional mantle reference line proposed in this study. However, a few data deviate from this trend, including zircon from two granulites from the Iisalmi region, central Finland (Lauri *et al.*, 2011), and these data require closer examination. Lauri *et al.* (2011) concluded that the existence of a few supra-chondritic initial ratios in single zircon is not clear evidence for a reservoir similar to the present-day depleted mantle, but interpret their data to support a chondritic to mildly supra-chondritic mantle reservoir. Importantly, all Karelian samples of Lauri *et al.* (2011) that give supra-chondritic initial zircon Hf isotope ratios are from zircon in granulite facies rocks that show evidence for unsupported radiogenic Pb, yielding $^{207}Pb/^{206}Pb$ dates that are spuriously old (see Whitehouse *et al.*, 2022). For example, reversely discordant data and an increase in the error ellipse caused by decoupling of the Pb and U signals are apparent in all these samples (see Lauri *et al.*, 2011). This is not uncommon in UHT (Ultra-High-Temperature) rocks and is interpreted to be caused by the formation of metallic Pb nanospheres (*e.g.*, Kusiak *et al.*, 2013; Whitehouse *et al.*, 2014). This clear correlation between unreliable age determinations and supra-chondritic initial zircon Hf isotope signatures, questions the geological significance of these few supra-chondritic signatures, and these analyses have hence been omitted from the compilation in Figure 2 (main manuscript).

Primitive *versus* felsic sources

To accurately interpret the crustal growth and evolution of the Fennoscandian Shield using zircon Lu-Hf isotope data requires a characterization of the mantle from which the crust was ultimately extracted. Even though zircon Hf isotope data from global compilations provide an important first order check and indicate a chondritic mantle from 4.5 Ga until *ca.* 3.5 Ga (*e.g.*, Voice *et al.*, 2011; Condie *et al.*, 2011; Belousova *et al.*, 2010; Dhuime *et al.*, 2012), these data are derived from silica-rich rocks that are not directly sourced from mantle peridotite (Reimink *et al.*, 2023). Hence, looking at the best preserved (*i.e.* least metamorphosed and altered), most primitive and mantle-derived rocks will provide a good complement, and a clearer insight to the chemical and isotopic composition of the mantle that underlies Fennoscandia. A characteristic feature of Fennoscandia is that existing data (especially for mafic rocks) show a restricted range in ε_{Hf} over a long period of time (*ca.* 2.8 Ga to 1.2 Ga), with compositions mostly scattering around and just above the chondritic reference (Fig. 4; Valbracht, 1991; Claesson and Lundqvist, 1995; Andersson *et al.*, 2006, 2007; Rutanen *et al.*, 2011; Petersson *et al.*, 2017). These previous studies interpret such Hf isotope data as evidence for mild time-

integrated depletion of the Fennoscandian mantle, perhaps reflecting <~2.3 Ga re-enrichment of depleted mantle as a result of long-term subduction beneath Fennoscandia (Andersen *et al.*, 2009a; Andersson *et al.*, 2011; Petersson *et al.*, 2015a, 2015b; Rutanen *et al.*, 2011). If the near chondritic isotope signatures in Paleoproterozoic mantle-derived mafic rocks in Fennoscandia represent long-term enrichment of a well-mixed upper mantle or SCLM (sub-continental-lithospheric-mantle), it is reasonable to assume that the mantle would have originally been more strongly depleted prior to the onset of this process. However, as noted by several studies (*e.g.*, Andersson *et al.*, 2006, 2007; Rutanen *et al.*, 2011; Petersson *et al.*, 2017), no Paleoproterozoic or older rocks in Fennoscandia show radiogenic Hf signatures that support derivation from a strongly depleted mantle source. We contend that this complicates a re-enrichment model, and that an alternative explanation for these isotope signatures is required. Several primitive intrusions in Fennoscandia negates a MORB depleted source, like the *ca.* 2.9 Ga Kuhmo komatiites and komatiitic basalts in the Karelian Province in eastern Finland (Svetov *et al.*, 2001), which have flat primitive mantle normalized trace-element patterns consistent with derivation from a mildly-depleted mantle source, less depleted than would be the case for a mantle reservoir back-calculated from modern radiogenic MORB (Hölttä *et al.*, 2014). The Al-undepleted signatures of these komatiites suggest derivation from a source more similar to a primitive upper mantle (Hölttä *et al.*, 2014). These signatures from primitive komatiites are compatible with a Paleo- to Mesoarchean chondritic mantle where the long-term extraction of continental crust was insufficient to cause long-term incompatible-element depletion in the upper mantle. The *ca.* 2.8 Ga Kostomuksha komatiites in western-most Russia, within the north-western parts of the Karelian Province, have whole-rock $\varepsilon_{Hf(t)}$ values that cluster tightly between +5.3 and +4.8 (Blichert-Toft and Puchtel, 2010), suggestive of a moderately depleted mantle (Fig. S-5). Similarly, 2.31 Ga dolerite dykes in the Lake Upper Kuito area in the Western Karelian province, give $\varepsilon_{Nd(t)}$ values of +0.5 to +0.8, just slightly above a chondritic composition (Stepanova *et al.*, 2015). Mafic plutonic, *ca.* 1.8 Ga rocks from the southern parts of the Fennoscandian Shield, that have $\varepsilon_{Nd(i)}$ just above CHUR and below a MORB-like depleted mantle, show no correlation between isotopic signatures and major element concentrations, *e.g.*, Mg# (Andersson *et al.*, 2007). The same lack of correlation between $\varepsilon_{Nd(i)}$ and Mg# and $\varepsilon_{Nd(i)}$ and $(Nb/La)_N$ is seen in 2.4 Ga basalts from the Karelian province (Bogina *et al.*, 2015), arguing against crustal contamination being responsible for lowering $\varepsilon_{Nd(i)}$ values. The Penikat layered intrusion, which is related to *ca.* 2.50 to 2.44 Ga plume magmatism in Finnish Lapland and the Kola Province has $^{87}Sr/^{86}Sr_{(i)}$ ranging between 0.7020 to 0.7040 (Luolavirta *et al.*, 2021) suggesting negligible contamination from crustal components in this mantle-derived ultramafic-mafic intrusion. Maier *et al.* (2018) similarly concluded that contamination with country rocks is not required in order to generate the chemical and isotopic signatures found in the Penikat intrusion. Additionally, a gabbro from the *ca.* 1.7 Ga Rymmen intrusion with $^{87}Sr/^{86}Sr_{(i)}$ indicative of mantle origin without crustal contamination (Claeson, 2002), and a coeval primitive gabbro from the Kleva intrusive complex, both from southern Sweden, give zircon $\varepsilon_{Hf(t)}$ signatures (Petersson *et al.*, 2017) that fall on the proposed *ca.* 3.5 Ga mantle evolution trend-line (Fig. 4). It is also noteworthy that even granitic rocks of the Transscandinavian Igneous Belt yield primitive $^{87}Sr/^{86}Sr_{(i)}$ between from 0.703 to 0.705 (see review by Högdahl *et al.*, 2004). Furthermore, in southern Sweden, at Norra Kärr, a *ca.* 1.5 Ga agpaitic nepheline syenite, which is interpreted to have evolved from a mantle source, yields zircon Hf isotope signatures with a mean $\varepsilon_{Hf(t)}$ value of *ca.* 7.5, equivalent to a moderately depleted source (Sjöqvist *et al.*, 2017). A few data points, at around 2.8 Ga (West Troms; Laurent *et al.*, 2019) and 1.9 Ga (Skellefteå; Guitreau *et al.*, 2014) do plot slightly above the proposed regional mantle evolution trend. However, as argued by Petersson *et al.* (2020), considering that laser ablation data typically have a reproducibility of ≥1.5 ε_{Hf} units (at 2 s.d.) when analysing REE-rich zircon (Fisher and Vervoort, 2018), data points plotting *ca.* 1.5 ε_{Hf} units above the true value are to be statistically expected. Hence, collectively, the isotopic signatures of the primitive and mantle derived rocks of Fennoscandia from 3.5 to 1.5 Ga suggest an uncontaminated, mildly depleted mantle source (Fig. S-5).

It is noteworthy that, when comparing the Hf isotope signatures from (ultra-)mafic and felsic rocks, their most radiogenic signatures fall more or less on the same line (Fig. S-5). While mafic and felsic rocks share an upper boundary of their most radiogenic signatures, the mafic rocks lack less radiogenic signatures (Fig. S-5). If, as argued above, the least fractionated, most primitive rocks in Fennoscandia mirror the isotope composition of the mantle source, then felsic rocks (zircon) giving matching signatures to the (ultra-)mafic rocks, is consistent with rapid differentiation from juvenile

mantle additions (basalts) to more evolved sialic compositions, as occurs in Phanerozoic ocean arc settings (see Kemp *et al.*, 2009). This is, however, not a feature restricted to Phanerozoic arcs, but can also be seen in the isotopic record of the Pilbara Craton, were Hf isotope compositions of (ultra-)mafic rocks have signatures only slightly more radiogenic than coeval TTGs, arguing for rapid reworking of juvenile mantle-derived crust (Kemp *et al.*, 2023).

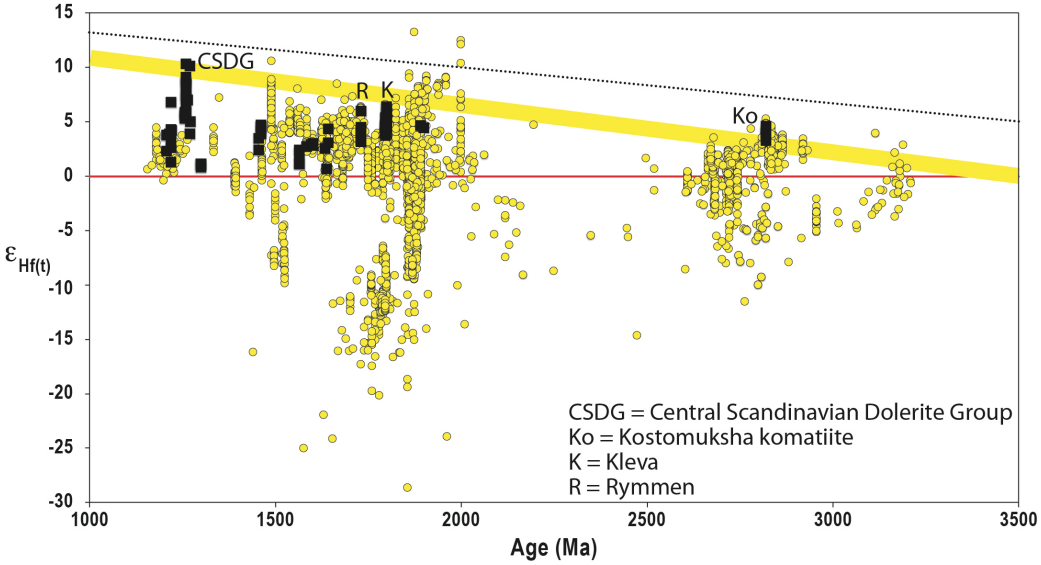

Figure S-5 Hf isotope data from primitive (black) and felsic (yellow) rocks of Fennoscandia.

Supplementary Tables

Table S-1 Zircon U-Pb isotope data.
Table S-2 Zircon O isotope data.
Table S-3 Zircon Lu-Hf isotope data.

Tables S-1 to S-3 are available for download (.xlsx) from the online version of this article at http://doi.org/10.7185/geochemlet.2435.

Supplementary Information References

Andersen, T., Andersson, U.B., Graham, S., Åberg, G., Simonsen, S.L. (2009a) Granitic magmatism by melting of juvenile continental crust: new constraints on the source of Palaeoproterozoic granitoids in Fennoscandia from Hf isotopes in zircon. *Journal of the Geological Society* 166, 233–247. https://doi.org/10.1144/0016-76492007-166

Andersson, U.B., Eklund, O., Fröjdö, S., Konopelko, D. (2006) 1.8 Ga magmatism in the Fennoscandian Shield; lateral variations in subcontinental mantle enrichment. *Lithos* 86, 110–136. https://doi.org/10.1016/j.lithos.2005.04.001

Andersson, U.B., Rutanen, H., Johansson, Å., Mansfeld, J., Rimša, A. (2007) Characterization of the Paleoproterozoic Mantle beneath the Fennoscandian Shield: Geochemistry and Isotope Geology (Nd, Sr) of ~ 1.8 Ga Mafic Plutonic Rocks from the Transscandinavian Igneous Belt in Southeast Sweden. *International Geology Review* 49, 587–625. https://doi.org/10.2747/0020-6814.49.7.587

Andersson, U.B., Begg, G.C., Griffin, W.L., Högdahl, K. (2011) Ancient and juvenile components in the continental crust and mantle: Hf isotopes in zircon from Svecofennian magmatic rocks and rapakivi granites in Sweden. *Lithosphere* 3, 409–419. https://doi.org/10.1130/L162.1

Appelquist, K., Cornell, D., Brander, L. (2008) Age, tectonic setting and petrogenesis of the Habo Volcanic Suite: Evidence for an active continental margin setting for the Transscandinavian Igneous Belt. *GFF* 130, 123–138. https://doi.org/10.1080/11035890809453228

Bejgarn, T., Söderlund, U., Weihed, P., Årebäck, H., Ernst, R.E. (2013) Palaeoproterozoic porphyry Cu–Au, intrusion-hosted Au and ultramafic Cu–Ni deposits in the Fennoscandian Shield: Temporal constraints using U–Pb geochronology. *Lithos* 174, 236–254. https://doi.org/10.1016/j.lithos.2012.06.015

Belousova, E.A., Kostitsyn, Y.A., Griffin, W.L., Begg, G.C., O'reilly, S.Y., Pearson, N.J. (2010) The growth of the continental crust: Constraints from zircon Hf-isotope data. *Lithos* 119, 457–466. https://doi.org/10.1016/j.lithos.2010.07.024

Bergman, S., Weihed, P. (2020) Archean (>2.6 Ga) and Paleoproterozoic (2.5–1.8 Ga), pre- and syn-orogenic magmatism, sedimentation and mineralization in the Norrbotten and Överkalix lithotectonic units, Svecokarelian orogen. In: Stephens, M.B., Bergman Weihed, J. (Eds.) *Sweden: Lithotectonic Framework, Tectonic Evolution and Mineral Resources*. Memoir 50, Geological Society of London, London, 27–82. https://doi.org/10.1144/M50-2016-29

Bergman, S., Kübler, L., Martinsson, O. (2001) *Description of regional geological and geophysical maps of northern Norrbotten County (east of the Caledonian orogen)*. Ba 56, Geological Survey of Sweden, Uppsala. https://resource.sgu.se/produkter/ba/ba56-beskrivning.pdf

Bergman, S., Billström, K., Persson, P.-O., Skiöld, T., Evins, P. (2006) U-Pb age evidence for repeated Palaeoproterozoic metamorphism and deformation near the Pajala shear zone in the northern Fennoscandian shield. *GFF* 128, 7–20. https://doi.org/10.1080/11035890601281007

Billström, K., Wasström, A., Bergström, U., Stigh, J. (2002) Age, geochemistry and crustal contamination of the Hemberget mafic-ultramafic layered intrusion in the Knaften area, northern Sweden. In: Bergman, S. (Ed.) *Radiometric dating results 5*, Research Paper C 834, Geological Survey of Sweden, Uppsala, 18–30. https://resource.sgu.se/produkter/c/c834-rapport.pdf

Bingen, B., Solli, A. (2009) Geochronology of magmatism in the Caledonian and Sveconorwegian belts of Baltica: synopsis for detrital zircon provenance studies. *Norwegian Journal of Geology* 89, 267–290. https://njg.geologi.no/images/NJG_articles/NGT_4_09_Bingen.pdf

Bingen, B., Nordgulen, Ø., Viola, G. (2008) A four-phase model for the Sveconorwegian orogeny, SW Scandinavia. *Norwegian Journal of Geology* 88, 43–72. https://njg.geologi.no/images/NJG_articles/Bingen_et_al_2_print.pdf

Björk. L., Kero. L. (1996) Bedrock map 22I Lycksele NW, SGU Ai 164 and in SGU. *Rapporter och meddelanden* 84, 72–75.

Blichert-Toft, J., Puchtel, I.S. (2010) Depleted mantle sources through time: Evidence from Lu–Hf and Sm–Nd isotope systematics of Archean komatiites. *Earth and Planetary Science Letters* 297, 598–606. https://doi.org/10.1016/j.epsl.2010.07.012

Bogdanova, S.V., Bingen, B., Gorbatschev, R., Kheraskova, T.N., Kozlov, V.I., Puchkov, V.N., Volozh, Yu.A. (2008) The East European Craton (Baltica) before and during the assembly of Rodinia. *Precambrian Research* 160, 23–45. https://doi.org/10.1016/j.precamres.2007.04.024

Bogina, M.M., Zlobin, V.L. Mints, M.V. (2015) Early Palaeoproterozoic volcanism of the Karelian Craton: age, sources, and geodynamic setting. *International Geology Review* 57, 1433–1445. https://doi.org/10.1080/00206814.2014.931783

Bouvier, A., Vervoort, J.D., Patchett, P.J. (2008) The Lu–Hf and Sm–Nd isotopic composition of CHUR: Constraints from unequilibrated chondrites and implications for the bulk composition of terrestrial planets. *Earth and Planetary Science Letters* 273, 48–57. https://doi.org/10.1016/j.epsl.2008.06.010

Brander, L., Söderlund, U. (2009) Mesoproterozoic (1.47–1.44 Ga) orogenic magmatism in Fennoscandia; Baddeleyite U–Pb dating of a suite of massif-type anorthosite in S. Sweden. *International Journal of Earth Sciences* 98, 499–516. https://doi.org/10.1007/s00531-007-0281-0

Claeson, D.T. (2002) Investigation of gabbroic rocks associated with the Småland-Värmland granitoid batholith of the Transscandinavian Igneous Belt, Sweden. Ph.D. thesis, Göteborgs Universitet.

Claesson, S., Lundqvist, T. (1995) Origins and ages of Proterozoic granitoids in the Bothnian Basin, central Sweden; isotopic and geochemical constraints. *Lithos* 36, 115–140. https://doi.org/10.1016/0024-4937(95)00010-D

Claesson, S., Huhma, H., Kinny, P.D., Williams, I.S. (1993) Svecofennian detrital zircon ages—implications for the Precambrian evolution of the Baltic Shield. *Precambrian Research* 64, 109–130. https://doi.org/10.1016/0301-9268(93)90071-9

Condie, K.C., Bickford, M.E., Aster, R.C., Belousova, E., Scholl, D.W. (2011) Episodic zircon ages, Hf isotopic composition, and the preservation rate of continental crust. *GSA Bulletin* 123, 951–957. https://doi.org/10.1130/B30344.1

Connelly, J.N., Berglund, J., Larson, S.Å. (1996) Thermotectonic evolution of the Eastern Segment of southwestern Sweden: tectonic constraints from U-Pb geochronology. In: Brewer, T.S. (Ed.) *Precambrian Crustal Evolution in the North Atlantic Region*. Geological Society, London, Special Publications 112, 297–313. https://doi.org/10.1144/GSL.SP.1996.112.01.16

Delin, H., Aaro, S. (1994) Bedrock map 17F Ånge SE, scale 1:50,000. *Sveriges geologiska undersökning* Ai 83.

Delin, H., Aaro, S. (2002) Bedrock map 17F Ånge NV, scale 1:50,000. *Sveriges geologiska undersökning* Ai 172.

Dhuime, B., Hawkesworth, C.J., Cawood, P.A. Storey, C.D. (2012) A Change in the Geodynamics of Continental Growth 3 Billion Years Ago. *Science* 335, 1334–1336. https://doi.org/10.1126/science.1216066

Fisher, C.M., Vervoort, J.D. (2018) Using the magmatic record to constrain the growth of continental crust—The Eoarchean zircon Hf record of Greenland. *Earth and Planetary Science Letters* 488, 79–91. https://doi.org/10.1016/j.epsl.2018.01.031

Fisher, C.M., Vervoort, J.D., DuFrane, S.A. (2014) Accurate Hf isotope determinations of complex zircons using the "laser ablation split stream" method. *Geochemistry, Geophysics, Geosystems* 15, 121–139. https://doi.org/10.1002/2013GC004962

Gaál, G., Gorbatschev, R. (1987) An Outline of the precambrian evolution of the baltic shield. *Precambrian Research* 35, 15–52. https://doi.org/10.1016/0301-9268(87)90044-1

González-Roldán, M.J. (2010) *Mineralogy, petrology and geochemistry of syn-volcanic intrusions in the Skellefte mining district, Northern Sweden*. Ph.D. thesis, Universidad de Huelva Departamento de Geología.

Guitreau, M., Blichert-Toft, J., Billström, K. (2014) Hafnium isotope evidence for early-Proterozoic volcanic arc reworking in the Skellefteå district (northern Sweden) and implications for the Svecofennian orogen. *Precambrian Research* 252, 39–52. https://doi.org/10.1016/j.precamres.2014.07.005

Haapala, I., Rämö, O.T., Frindt, S. (2005) Comparison of Proterozoic and Phanerozoic rift-related basaltic-granitic magmatism. *Lithos* 80, 1–32. https://doi.org/10.1016/j.lithos.2004.04.057

Hermansson, T., Stephens, M.B., Corfu, F., Page, L.M., Andersson, J. (2008) Migratory tectonic switching, western Svecofennian orogen, central Sweden: Constraints from U/Pb zircon and titanite geochronology. *Precambrian Research* 161, 250–278. https://doi.org/10.1016/j.precamres.2007.08.008

Hubbard, F.H. (1975) The Precambrian crystalline complex of south-western Sweden. The geology and petrogenetic development of the Varberg region. *GFF* 97, 223–236. https://doi.org/10.1080/11035897509454305

Högdahl, K., Andersson, U.B., Eklund, O. (Eds.) (2004) *The Transscandinavian Igneous Belt (TIB) in Sweden: a review of its character and evolution*. Special Paper 37, Geological Survey of Finland, Espoo.

Högdahl, K., Majka, J., Sjöström, H., Nilsson, K.P., Claesson, S., Konečný, P. (2012) Reactive monazite and robust zircon growth in diatexites and leucogranites from a hot, slowly cooled orogen: implications for the Palaeoproterozoic tectonic evolution of the central Fennoscandian Shield, Sweden. *Contributions to Mineralogy and Petrology* 163, 167–188. https://doi.org/10.1007/s00410-011-0664-x

Hölttä, P., Heilimo, E., Huhma, H., Kontinen, A., Mertanen, S., Mikkola, P., Paavlova, J., Peltonen, P., Semprich, J., Salbunov, A., Sorjonen-Ward, P. (2014) The Archaean Karelia and Belomorian Provinces, Fennoscandian Shield. In: Dilek, Y., Furnes, H. (Eds.) *Evolution of Archean Crust and Early Life*. Modern Approaches in Solid Earth Sciences, vol. 7, Springer, Dordrecht, 55–102. https://doi.org/10.1007/978-94-007-7615-9_3

Jaffey, A.H., Flynn, K.F., Glendenin, L.E., Bentley, W.C., Essling, A.M. (1971) Precision Measurement of Half-Lives and Specific Activities of ^{235}U and ^{238}U. *Physical Review C* 4, 1889. https://doi.org/10.1103/PhysRevC.4.1889

Johansson, Å., Waight, T., Andersen, T., Simonsen, S.L. (2016) Geochemistry and petrogenesis of Mesoproterozoic A-type granitoids from the Danish island of Bornholm, southern Fennoscandia. *Lithos* 244, 94–108. https://doi.org/10.1016/j.lithos.2015.11.031

Kärki, A., Laajoki, K., Luukas, J. (1993) Major Palaeoproterozoic shear zones of the central Fennoscandian Shield. *Precambrian Research* 64, 207–223. https://doi.org/10.1016/0301-9268(93)90077-F

Kemp, A.I.S., Foster, G.L., Scherstén, A., Whitehouse, M.J., Darling, J., Storey, C. (2009) Concurrent Pb–Hf isotope analysis of zircon by laser ablation multi-collector ICP-MS, with implications for the crustal evolution of Greenland and the Himalayas. *Chemical Geology* 261, 244–260. https://doi.org/10.1016/j.chemgeo.2008.06.019

Kemp, A.I.S., Vervoort, J.D., Bjorkman, K.E., Iaccheri, L.M. (2017) Hafnium Isotope Characteristics of Palaeoarchaean Zircon OG1/OGC from the Owens Gully Diorite, Pilbara Craton, Western Australia. *Geostandards and Geoanalytical Research* 41, 659–673. https://doi.org/10.1111/ggr.12182

Kemp, A.I.S., Vervoort, J.D., Petersson, A., Smithies, R.H., Lu, Y. (2023) A linked evolution for granite-greenstone terranes of the Pilbara Craton from Nd and Hf isotopes, with implications for Archean continental growth. *Earth and Planetary Science Letters* 601, 117895. https://doi.org/10.1016/j.epsl.2022.117895

Korja, A., Lahtinen, R., Nironen, M. (2006) The Svecofennian orogen: a collage of microcontinents and island arcs. In: Gee, D.G., Stephenson, R.A. (Eds.) *European Lithosphere Dynamics*. Memoir 32, Geological Society, London, 561–578. https://doi.org/10.1144/GSL.MEM.2006.032.01.34

Kusiak, M.A., Whitehouse, M.J., Wilde, S.A., Nemchin, A.A., Clark, C. (2013) Mobilization of radiogenic Pb in zircon revealed by ion imaging: Implications for early Earth geochronology. *Geology* 41, 291–294. https://doi.org/10.1130/G33920.1

Laurent, O., Vander Auwera, J., Bingen, B., Bolle, O., Gerdes, A. (2019) Building up the first continents: Mesoarchean to Paleoproterozoic crustal evolution in West Troms, Norway, inferred from granitoid petrology, geochemistry and zircon U-Pb/Lu-Hf isotopes. *Precambrian Research* 321, 303–327. https://doi.org/10.1016/j.precamres.2018.12.020

Lauri, L.S., Andersen, T., Hölttä, P., Huhma, H., Graham, S. (2011) Evolution of the Archaean Karelian Province in the Fennoscandian Shield in the light of U–Pb zircon ages and Sm–Nd and Lu–Hf isotope systematics. *Journal of the Geological Society* 168, 201–218. https://doi.org/10.1144/0016-76492009-159

Ludwig, K.R. (2008) Isoplot 3.70. A Geochronological Toolkit for Microsoft Excel. *Berkeley Geochronology Center Special Publication* 4.

Lundqvist, T., Lundin. A. (1999) Rapporter och Meddelanden, *SGU-RM* 98, 91–104.

Lundqvist, T., Vaasjoki, M., Skiöld, T. (1996) Preliminary note on the occurrence of Archaean rocks in the Vallen–Alhamn area, northern Sweden. In: Lundqvist, T. (Ed.) *Radiometric dating results 2*. SGU series C, Research Paper 828, Geological Survey of Sweden, Uppsala, 32–33. https://resource.sgu.se/dokument/publikation/c/c828rapport/c828-rapport.pdf

Lundqvist, T., Vaasjoki, M., Persson, P.-O. (1998) U-Pb ages of plutonic and volcanic rocks in the Svecofennian Bothnian Basin, central Sweden, and their implications for the Palaeoproterozoic evolution of the basin. *GFF* 120, 357–363. https://doi.org/10.1080/11035899801204357

Lundqvist, T., Skiöld, T., Vaasjoki, M. (2000) Archaean–Proterozoic geochronology of the Vallen-Alhamn area, northern Sweden. *GFF* 122, 273–280. https://doi.org/10.1080/11035890001223273

Luolavirta, K., Yang, S.H., Rivas, I., Vähätiitto, J., Lahaye, Y., Maier, W. (2021) Sr isotope and trace-element characteristics of Finnish Layered intrusions; In-situ Sr isotope study of the Penikat intrusion, northern Finland. *ARLIN – Online Workshop* 1, Apatity, February 25, 2021. https://doi.org/10.31241/ARLIN.2021.013

Maier, W.D., Halkoaho, T., Huhma, H., Hanski, E., Barnes, S.-J. (2018) The Penikat Intrusion, Finland: Geochemistry, Geochronology, and Origin of Platinum–Palladium Reefs. *Journal of Petrology* 59, 967–1006. https://doi.org/10.1093/petrology/egy051

Mellqvist, C., Öhlander, B., Weihed, P., Schöberg, H. (2003) Some aspects on the subdivision of the Haparanda and Jörn intrusive suites in northern Sweden. *GFF* 125, 77–85. https://doi.org/10.1080/11035890301252077

Mercier-Langevin, P., McNicoll, V., Allen, R.L., Blight, J.H.S., Dubé, B. (2013) The Boliden gold-rich volcanogenic massive sulfide deposit, Skellefte district, Sweden: new U–Pb age constraints and implications at deposit and district scale. *Mineralum Deposita* 48, 485–504. https://doi.org/10.1007/s00126-012-0438-z

Nasdala, L., Hofmeister, W., Norberg, N., Martinson, J.M., Corfu, F., Dörr, W., Kamo, S.L., Kennedy, A.K., Kronz, A., Reiners, P.W., Frei, D., Kosler, J., Wan, Y., Götze, J., Häger, T., Kröner, A., Valley, J.W. (2008) Zircon M257 - a Homogeneous Natural Reference Material for the Ion Microprobe U-Pb Analysis of Zircon. *Geostandards and Geoanalytical Research* 32, 247–265. https://doi.org/10.1111/j.1751-908X.2008.00914.x

Öhlander, B., Schöberg, H. (1991) Character and U-Pb zircon age of the Proterozoic Ale granite, northern Sweden. *GFF* 113, 105–112. https://doi.org/10.1080/11035899109453843

Petersson, A., Scherstén, A., Andersson, J., Möller, C. (2015) Zircon U–Pb and Hf-isotopes from the eastern part of the Sveconorwegian Orogen, SW Sweden: implications for the growth of Fennoscandia. In: Roberts, N.M.W., Van Kranendonk,

M., Parman, S., Shirey, S., Clift, P.D. (Eds.) *Continent Formation Through Time*. Geological Society, London, Special Publications 389, 281–303. https://doi.org/10.1144/SP389.2

Petersson, A., Scherstén, A., Bingen, B., Gerdes, A., Whitehouse, M.J. (2015b) Mesoproterozoic continental growth: U–Pb–Hf–O zircon record in the Idefjorden Terrane, Sveconorwegian Orogen. *Precambrian Research* 261, 75–95. https://doi.org/10.1016/j.precamres.2015.02.006

Petersson, A., Björnborg, K., Scherstén, A., Gerdes, A. Næraa, T. (2017) Tracing Proterozoic arc mantle Hf isotope depletion of southern Fennoscandia through coupled zircon U–Pb and Lu–Hf isotopes. *Lithos* 284–285, 122–131. https://doi.org/10.1016/j.lithos.2017.04.010

Petersson, A., Kemp, A.I.S., Hickman, A.H., Whitehouse, M.J., Martin, L., Gray, C.M. (2019a) A new 3.59 Ga magmatic suite and a chondritic source to the east Pilbara Craton. *Chemical Geology* 511, 51–70. https://doi.org/10.1016/j.chemgeo.2019.01.021

Petersson, A., Kemp, A.I.S., Gray, C.M., Whitehouse, M.J. (2020) Formation of early Archean Granite-Greenstone Terranes from a globally chondritic mantle: Insights from igneous rocks of the Pilbara Craton, Western Australia. *Chemical Geology* 551, 119757. https://doi.org/10.1016/j.chemgeo.2020.119757

Petersson, A., Waight, T., Kemp, A.I.S., Whitehouse, M.J., Valley, J.W. (2024a) An Eoarchean continental nucleus for the Fennoscandian Shield and a link to the North Atlantic craton. *Geology* 52, 171–175. https://doi.org/10.1130/G51658.1

Reimink, J.R., Davies, J.H.F.L., Moyen, J.-F., Pearson, D.G. (2023) A whole-lithosphere view of continental growth. *Geochemical Perspectives Letters* 26, 45–49. https://doi.org/10.7185/geochemlet.2324

Rimša, A., Johansson, L., Whitehouse, M.J. (2007) Constraints on incipient charnockite formation from zircon geochronology and rare earth element characteristics. *Contributions to Mineralogy and Petrology* 154, 357–369. https://doi.org/10.1007/s00410-007-0197-5

Romer, R.L., Smeds, S.-A. (1997) U–Pb columbite chronology of post-kinematic Palaeoproterozoic pegmatites in Sweden. *Precambrian Research* 82, 85–99. https://doi.org/10.1016/S0301-9268(96)00050-2

Rudnick, R.L., Gao, S. (2003) 3.01 - Composition of the Continental Crust. In: Holland, H.D., Turekian, K.K. (Eds.) *Treatise on Geochemistry*. First Edition, Elsevier, Amsterdam, 1–64. https://doi.org/10.1016/B0-08-043751-6/03016-4

Rutanen, H., Andersson, U.B., Väisänen, M., Johansson, Å., Fröjdö, S., Lahaye, Y., Eklund, O. (2011) 1.8 Ga magmatism in southern Finland: strongly enriched mantle and juvenile crustal sources in a post-collisional setting. *International Geology Review* 53, 1622–1683. https://doi.org/10.1080/00206814.2010.496241

Rutland, R.W.R., Skiöld, T., Page, R.W. (2001) Age of deformation episodes in the Palaeoproterozoic domain of northern Sweden, and evidence for a pre-1.9 Ga crustal layer. *Precambrian Research* 112, 239–259. https://doi.org/10.1016/S0301-9268(01)00166-8

Sadeghi, M., Hellström, F. (2018) *U-Pb zircon age of an Archean granodioritic gneiss in the Boden area, northern Sweden*. SGU-rapport 2018:03, Geological Survey of Sweden, Uppsala. https://resource.sgu.se/dokument/publikation/sgurapport/sgurapport201803rapport/s1803-rapport.pdf

Scherer, E., Münker, C., Mezger, K. (2001) Calibration of the Lutetium-Hafnium Clock. *Science* 293, 683–687. https://doi.org/10.1126/science.1061372

Segal, I., Halicz, L., Platzner, I.T. (2003) Accurate isotope ratio measurements of ytterbium by multiple collection inductively coupled plasma mass spectrometry applying erbium and hafnium in an improved double external normalization procedure. *Journal of Analytical Atomic Spectrometry* 18, 1217–1223. https://doi.org/10.1039/b307016f

Sjöqvist, A.S.L., Cornell, D.H., Andersen, T., Christensson, U.I., Berg, J.T. (2017) Magmatic age of rare-earth element and zirconium mineralisation at the Norra Kärr alkaline complex, southern Sweden, determined by U–Pb and Lu–Hf isotope analyses of metasomatic zircon and eudialyte. *Lithos* 294–295, 73–86. https://doi.org/10.1016/j.lithos.2017.09.023

Skyttä, P., Weihed, P., Högdahl, K., Bergman, S., Stephens, M.B. (2020) Paleoproterozoic (2.0–1.8 Ga) syn-orogenic sedimentation, magmatism and mineralization in the Bothnia–Skellefteå lithotectonic unit, Svecokarelian orogen. In: Stephens, M.B., Bergman Weihed, J. (Eds.) *Sweden: Lithotectonic Framework, Tectonic Evolution and Mineral Resources*. Geological Society, London, Memoirs 50, 83–130. https://doi.org/10.1144/M50-2017-10

Söderlund, U., Jarl, L.-G., Persson, P.-O., Stephens, M.B., Wahlgren, C.-H. (1999) Protolith ages and timing of deformation in the eastern, marginal part of the Sveconorwegian orogen, southwestern Sweden. *Precambrian Research* 94, 29–48. https://doi.org/10.1016/S0301-9268(98)00104-1

Söderlund, U., Möller, C., Andersson, J., Johansson, L. Whitehouse, M. (2002) Zircon geochronology in polymetamorphic gneisses in the Sveconorwegian orogen, SW Sweden: ion microprobe evidence for 1.46–1.42 and 0.98–0.96 Ga reworking. *Precambrian Research* 113, 193–225. https://doi.org/10.1016/S0301-9268(01)00206-6

Söderlund, U., Patchett, P.J., Vervoort, J.D., Isachsen, C.E. (2004) The ^{176}Lu decay constant determined by Lu–Hf and U–Pb isotope systematics of Precambrian mafic intrusions. *Earth and Planetary Science Letters* 219, 311–324. https://doi.org/10.1016/S0012-821X(04)00012-3

Söderlund, U., Hellström, F.A., Kamo, S.L. (2008) Geochronology of high-pressure mafic granulite dykes in SW Sweden: tracking the *P–T–t* path of metamorphism using Hf isotopes in zircon and baddeleyite. *Journal of Metamorphic Geology* 26, 539–560. https://doi.org/10.1111/j.1525-1314.2008.00776.x

Stacey, J.T., Kramers, J.D. (1975) Approximation of terrestrial lead isotope evolution by a two-stage model. *Earth and Planetary Science Letters* 26, 207–221. https://doi.org/10.1016/0012-821X(75)90088-6

Steiger, R.H., Jäger, E. (1977) Subcommission on geochronology: Convention on the use of decay constants in geo- and cosmochronology. *Earth and Planetary Science Letters* 36, 359–362. https://doi.org/10.1016/0012-821X(77)90060-7

Stepanova, A.V., Salnikova, E.B., Samsonov, A.V., Egorova, S.V., Larionova, Y.O., Stepanov, V.S. (2015) The 2.31 Ga mafic dykes in the Karelian Craton, eastern Fennoscandian shield: U–Pb age, source characteristics and implications for continental break-up processes. *Precambrian Research* 259, 43–57. https://doi.org/10.1016/j.precamres.2014.10.002

Stephens, M.B. (2009) *Synthesis of the bedrock geology in the Bergslagen region, Fennoscandian Shield, south-central Sweden*. Serie Ba, Översiktskartor med beskrivningar, Geological Survey of Sweden, Uppsala.

Stephens, M.B. (2020) Introduction to the lithotectonic framework of Sweden and organization of this Memoir. In: Stephens, M.B., Bergman Weihed, J. (Eds.) *Sweden: Lithotectonic Framework, Tectonic Evolution and Mineral Resources*. Geological Society, London, Memoirs 50, 1–15. https://doi.org/10.1144/M50-2019-21

Stephens, M.B., Bergman, S. (2020) Regional context and lithotectonic framework of the 2.0–1.8 Ga Svecokarelian orogen, eastern Sweden. In: Stephens, M.B., Bergman Weihed, J. (Eds.) *Sweden: Lithotectonic Framework, Tectonic Evolution and Mineral Resources*. Geological Society, London, Memoirs 50, 19–26. https://doi.org/10.1144/M50-2017-2

Svetov, S.A., Svetova, A.I., Huhma, H. (2001) Geochemistry of the Komatiite-Tholeiite Rock Association in the Vedlozero-Segozero Archean Greenstone Belt, Central Karelia. *Geochemistry International* 39, Suppl. 1, S24–S38.

Valbracht, P.J. (1991) Early Proterozoic continental tholeiites from western Bergslagen, Central Sweden, II. Nd and Sr isotopic variations and implications from Sm–Nd systematics for the Svecofennian sub-continental mantle. *Precambrian Research* 52, 215–230. https://doi.org/10.1016/0301-9268(91)90081-K

Valley, J.W., Lackey, J.S., Cavosie, A.J., Clechenko, C.C., Spicuzza, M.J., Basei, M.A.S., Bindeman, I.N., Ferreira, V.P., Sial, A.N., King, E.M., Peck, W.H., Sinha, A.K., Wei, C.S. (2005) 4.4 billion years of crustal maturation: oxygen isotope ratios of magmatic zircon. *Contributions to Mineralogy and Petrology* 150, 561–580. https://doi.org/10.1007/s00410-005-0025-8

Vervoort, J.D., Patchett, P.J. (1996) Behavior of hafnium and neodymium isotopes in the crust: Constraints from Precambrian crustally derived granites. *Geochimica et Cosmochimica Acta* 60, 3717–3733. https://doi.org/10.1016/0016-7037(96)00201-3

Vervoort, J.D., Patchett, P.J., Söderlund, U., Baker, M. (2004) Isotopic composition of Yb and the determination of Lu concentrations and Lu/Hf ratios by isotope dilution using MC-ICPMS. *Geochemistry, Geophysics, Geosystems* 5, Q11002. https://doi.org/10.1029/2004GC000721

Voice, P.J., Kowalewski, M., Eriksson, K.A. (2011) Quantifying the Timing and Rate of Crustal Evolution: Global Compilation of Radiometrically Dated Detrital Zircon Grains. *The Journal of Geology* 119, 109–126. https://doi.org/10.1086/658295

Waight, T.E., Frei, D., Storey, M. (2012) Geochronological constraints on granitic magmatism, deformation, cooling and uplift on Bornholm, Denmark. *Bulletin of the Geological Society of Denmark* 60, 23–46. https://doi.org/10.37570/bgsd-2012-60-03

Wasström, A. (1993) The Knaften granitoids of Västerbotten County, northern Sweden. In: Lundqvist, T. (Ed.) *Radiometric dating results*. SGU series C, Research Paper 823, Geological Survey of Sweden, Uppsala, 60–64. https://resource.sgu.se/dokument/publikation/c/c823rapport/c823-rapport.pdf

Wasström, A., Huhma, H., Lahtinen, R., Andersson, J., Hellström, F. (2019) Pre-1.94 to post-1.88 Ga sediment depositional environment and c. 1.94 Ga felsic magmatism in the Knaften area, northern Sweden. *GFF* 141, 21–39. https://doi.org/10.1080/11035897.2019.1569126

Weihed, P., Billström, K., Persson, P.O., Bergman Weihed, J. (2002) Relationship between 1.90–1.85 Ga accretionary processes and 1.82–1.80 Ga oblique subduction at the Karelian craton margin, Fennoscandian Shield. *GFF* 124, 163–180. https://doi.org/10.1080/11035890201243163

Weihed, P., Arndt, N., Billström, K., Duchesne, J.-C., Eilu, P., Martinsson, O., Papunen, H., Lahtinen, R. (2005) 8: Precambrian geodynamics and ore formation: The Fennoscandian Shield. *Ore Geology Reviews* 27, 273–322. https://doi.org/10.1016/j.oregeorev.2005.07.008

Welin, E., Christansson, K., Kähr, A.-M. (1993) Isotopic investigations of metasedimentary and igneous rocks in the Palaeoproterozoic Bothnian Basin, central Sweden. *GFF* 115, 285–296. https://doi.org/10.1080/11035899309453915

Whitehouse, M.J., Kamber, B.S. (2005) Assigning Dates to Thin Gneissic Veins in High-Grade Metamorphic Terranes: A Cautionary Tale from Akilia, Southwest Greenland. *Journal of Petrology* 46, 291–318. https://doi.org/10.1093/petrology/egh075

Whitehouse, M.J., Kamber, B.S., Moorbath, S. (1999) Age significance of U–Th–Pb zircon data from early Archaean rocks of west Greenland—a reassessment based on combined ion-microprobe and imaging studies. *Chemical Geology* 160, 201–224. https://doi.org/10.1016/S0009-2541(99)00066-2

Whitehouse, M.J., Ravindra Kumar, G.R., Rimša, A. (2014) Behaviour of radiogenic Pb in zircon during ultrahigh-temperature metamorphism: an ion imaging and ion tomography case study from the Kerala Khondalite Belt, southern India. *Contributions to Mineralogy and Petrology* 168, 1042. https://doi.org/10.1007/s00410-014-1042-2

Whitehouse, M.J., Kemp, A.I.S., Petersson, A. (2022) Persistent mildly supra-chondritic initial Hf in the Lewisian Complex, NW Scotland: Implications for Neoarchean crust-mantle differentiation. *Chemical Geology* 606, 121001. https://doi.org/10.1016/j.chemgeo.2022.121001

Wiedenbeck, M., Hanchar, J.M., Peck, W.H., Sylvester, P., Valley, J., Whitehouse, M., Kronz, A., Morishita, Y., Nasdala, L., Fiebig, J., Franchi, I., Girard, J.-P., Greenwood, R.C., Hinton, R., Kita, N., Mason, P.R.D., Norman, M., Ogasawara, M., Piccoli, P.M., Rhede, D., Satoh, H., Schulz-Dobrick, B., Skar, O., Spicuzza, M.J., Terada, K., Tindle, A., Togashi, S., Vennemann, T., Xie, Q., Zheng, Y.-F. (2004) Further Characterisation of the 91500 Zircon Crystal. *Geostandards and Geoanalytical Research* 28, 9–39. https://doi.org/10.1111/j.1751-908X.2004.tb01041.x

Wikström, A. (1996) U–Pb zircon dating of a coarse porphyritic quartz monzonite and an even grained, grey tonalitic gneiss from the Tiveden area, south central Sweden. In: Lundqvist, T. (Ed.) *Radiometric dating results 2*. SGU series C, Research Paper 828, Geological Survey of Sweden, Uppsala, 41-47. https://resource.sgu.se/dokument/publikation/c/c828rapport/c828-rapport.pdf

Wilson, M.R., Hamilton, P.J., Fallick, A.E., Aftalion, M., Michard, A. (1985) Granites and early Proterozoic crustal evolution in Sweden: evidence from Sm–Nd, U–Pb and O isotope systematics. *Earth and Planetary Science Letters* 72, 376–388. https://doi.org/10.1016/0012-821X(85)90059-7

Woodhead, J.D., Hergt, J.M. (2005) A Preliminary Appraisal of Seven Natural Zircon Reference Materials for *In Situ* Hf Isotope Determination. *Geostandards and Geoanalytical Research* 29, 183–195. https://doi.org/10.1111/j.1751-908X.2005.tb00891.x

References for Zircon/baddeleyite Lu-Hf Isotope Data from Fennoscandia

Andersen, T., Griffin, W.L., Pearson, N.J. (2002) Crustal Evolution in the SW Part of the Baltic Shield: the Hf Isotope Evidence. *Journal of Petrology* 43, 1725–1747. https://doi.org/10.1093/petrology/43.9.1725

Andersen, T., Griffin, W.L., Jackson, S.E., Knudsen, T.-L., Pearson, N.J. (2004) Mid-Proterozoic magmatic arc evolution at the southwest margin of the Baltic shield. *Lithos* 73, 289–318. https://doi.org/10.1016/j.lithos.2003.12.011

Andersen, T., Griffin, W.L., Sylvester, A.G. (2007) Sveconorwegian crustal underplating in southwestern Fennoscandia. LAM-ICPMS U–Pb and Lu–Hf isotope evidence from granites and gneisses in Telemark, southern Norway. *Lithos* 93, 273–287. https://doi.org/10.1016/j.lithos.2006.03.068

Andersen, T., Andersson, U.B., Graham, S., Åberg, G., Simonsen, S.L. (2009a) Granitic magmatism by melting of juvenile continental crust: new constraints on the source of Palaeoproterozoic granitoids in Fennoscandia from Hf isotopes in zircon. *Journal of the Geological Society* 166, 233–247. https://doi.org/10.1144/0016-76492007-166

Andersen, T., Graham, S., Sylvester, A.G. (2009b) The geochemistry, Lu–Hf isotope systematics, and petrogenesis of late Mesoproterozoic A-type granites in southwestern Fennoscandia. *Canadian Mineralogist* 47, 1399–1422. https://doi.org/10.3749/canmin.47.6.1399

Andersson, U.B., Begg, G.C., Griffin, W.L., Högdahl, K. (2011) Ancient and juvenile components in the continental crust and mantle: Hf isotopes in zircon from Svecofennian magmatic rocks and rapakivi granites in Sweden. *Lithosphere* 3, 409–419. https://doi.org/10.1130/L162.1

Bingen, B., Belousova, E.A., Griffin, W.L. (2011) Neoproterozoic recycling of the Sveconorwegian orogenic belt. Detrital-zircon data from the Sparagmite basins in the Scandinavian Caledonides. *Precambrian Research* 189, 347–367. https://doi.org/10.1016/j.precamres.2011.07.005

Brander, L., Söderlund, U., Bingen, B. (2011) Tracing the 1271–1246 Ma Central Scandinavian Dolerite Group mafic magmatism in Fennoscandia: U–Pb baddeleyite and Hf isotope data on the Moslätt and Børgefjell dolerites. *Geological Magazine* 148, 632–643. https://doi.org/10.1017/S0016756811000033

Brewer, T.S., Åhäll, K.-I., Menuge, J.F., Storey, C.D., Parrish, R.R. (2004) Mesoproterozoic bimodal volcanism in SW Norway, evidence for recurring pre-Sveconorwegian continental margin tectonism. *Precambrian Research* 134, 249–273. https://doi.org/10.1016/j.precamres.2004.06.003

Heilimo, E., Halla, J., Andersen, T., Huhma, H. (2013) Neoarchean crustal recycling and mantle metasomatism: Hf–Nd–Pb–O isotope evidence from sanukitoids of the Fennoscandian shield. *Precambrian Research* 228, 250–266. https://doi.org/10.1016/j.precamres.2012.01.015

Heinonen, A.P., Andersen, T., Rämö, O.T. (2010) Re-evaluation of Rapakivi Petrogenesis: Source Constraints from the Hf Isotope Composition of Zircon in the Rapakivi Granites and Associated Mafic Rocks of Southern Finland. *Journal of Petrology* 51, 1687–1709. https://doi.org/10.1093/petrology/egq035

Heinonen, A., Andersen, T., Rämö, O.T., Whitehouse, M. (2015) The source of Proterozoic anorthosite and rapakivi granite magmatism: evidence from combined *in situ* Hf–O isotopes of zircon in the Ahvenisto complex, southeastern Finland. *Journal of the Geological Society* 172, 103–112. https://doi.org/10.1144/jgs2014-013

Johansson, Å. (2021) Cleaning up the record – revised U-Pb zircon ages and new Hf isotope data from southern Sweden. *GFF* 143, 328–359. https://doi.org/10.1080/11035897.2021.1939777

Johansson, Å., Andersen, T., Simonsen, S.L. (2015) Hafnium isotope characteristics of late Palaeoproterozoic magmatic rocks from Blekinge, southeast Sweden: possible correlation of small-scale Hf and Nd isotope variations in zircon and whole rocks. *GFF* 137, 74–82. https://doi.org/10.1080/11035897.2014.992469

Kara, J., Väisänen, M., Johansson, Å., Lahaye, Y., O'Brien, H., Eklund, O. (2018) 1.90-1.88 Ga arc magmatism of central Fennoscandia. geochemistry, U-Pb geochronology, Sm-Nd and Lu-Hf isotope systematics of plutonicvolcanic rocks from southern Finland. *Geologica Acta* 16, 1–23. https://doi.org/10.1344/GeologicaActa2018.16.1.1

Kara, J., Väisänen, M., Heinonen, J.S., Lahaye, Y., O'Brien, H., Huhma, H. (2020) Tracing arclogites in the Paleoproterozoic Era – A shift from 1.88 Ga calc-alkaline to 1.86 Ga high-Nb and adakite-like magmatism in central Fennoscandian Shield. *Lithos* 372–373, 105663. https://doi.org/10.1016/j.lithos.2020.105663

Kara, J., Leskelä, T., Väisänen, M., Skyttä, P., Lahaye, Y., Tiainen, M., Leväniemi, H. (2021) Early Svecofennian rift-related magmatism: Geochemistry, U-Pb-Hf zircon isotope data and tectonic setting of the Au-hosting Uunimäki gabbro, SW Finland. *Precambrian Research* 364, 106364. https://doi.org/10.1016/j.precamres.2021.106364

Lamminen, J., Andersen, T., Nystuen, J.P. (2011) Zircon U-Pb ages and Lu-Hf isotopes from basement rocks associated with Neoproterozoic sedimentary successions in the Sparagmite Region and adjacent areas, South Norway: the crustal architecture of western Baltica. *Norwegian Journal of Geology* 91, 35–55. https://njg.geologi.no/images/NJG_articles/NJG_1_2_2011_Lamminen_etal_pr.pdf

Laurent, O., Vander Auwera, J., Bingen, B., Bolle, O., Gerdes, A. (2019) Building up the first continents: Mesoarchean to Paleoproterozoic crustal evolution in West Troms, Norway, inferred from granitoid petrology, geochemistry and zircon U-Pb/Lu-Hf isotopes. *Precambrian Research* 321, 303–327. https://doi.org/10.1016/j.precamres.2018.12.020

Lauri, L.S., Andersen, T., Hölttä, P., Huhma, H., Graham, S. (2011) Evolution of the Archaean Karelian Province in the Fennoscandian Shield in the light of U–Pb zircon ages and Sm–Nd and Lu–Hf isotope systematics. *Journal of the Geological Society* 168, 201–218. https://doi.org/10.1144/0016-76492009-159

Lauri, L.S., Andersen, T., Räsänen, J., Juopperi, H. (2012) Temporal and Hf isotope geochemical evolution of southern Finnish Lapland from 2.77 Ga to 1.76 Ga. *Bulletin of the Geological Society of Finland* 84, 121–140. https://doi.org/10.17741/bgsf/84.2.002

Patchett, P.J., Kouvo, O., Hedge, C.E., Tatsumoto, M. (1982) Evolution of continental crust and mantle heterogeneity: Evidence from Hf isotopes. *Contributions to Mineralogy and Petrology* 78, 279–297. https://doi.org/10.1007/BF00398923

Pedersen, S., Andersen, T., Konnerup-Madsen, J., Griffin, W.L. (2009) Recurrent Mesoproterozoic continental magmatism in South-Central Norway. *International Journal of Earth Sciences* 98, 1151–1171. https://doi.org/10.1007/s00531-008-0309-0

Petersson, A., Tual, L. (2020) Zircon U–Pb-Hf isotope data in eclogite and metagabbro from southern Sweden reveal a common long-lived evolution and enriched source. *GFF* 142, 253–266. https://doi.org/10.1080/11035897.2020.1822438

Petersson, A., Scherstén, A., Andersson, J., Möller, C. (2015a) Zircon U–Pb and Hf – isotopes from the eastern part of the Sveconorwegian Orogen, SW Sweden: implications for the growth of Fennoscandia. In: Roberts, N.M.W., Van Kranendonk, M., Parman, S., Shirey, S., Clift, P.D. (Eds.) *Continent Formation Through Time*. Geological Society, London, Special Publications 389, 281–303. https://doi.org/10.1144/SP389.2

Petersson, A., Scherstén, A., Bingen, B., Gerdes, A., Whitehouse, M.J. (2015b) Mesoproterozoic continental growth: U–Pb–Hf–O zircon record in the Idefjorden Terrane, Sveconorwegian Orogen. *Precambrian Research* 261, 75–95. https://doi.org/10.1016/j.precamres.2015.02.006

Petersson, A., Bjärnborg, K., Scherstén, A., Gerdes, A. Næraa, T. (2017) Tracing Proterozoic arc mantle Hf isotope depletion of southern Fennoscandia through coupled zircon U–Pb and Lu–Hf isotopes. *Lithos* 284–285, 122–131. https://doi.org/10.1016/j.lithos.2017.04.010

Sjöqvist, A.S.L., Cornell, D.H., Andersen, T., Christensson, U.I., Berg, J.T. (2017) Magmatic age of rare-earth element and zirconium mineralisation at the Norra Kärr alkaline complex, southern Sweden, determined by U–Pb and Lu–Hf isotope analyses of metasomatic zircon and eudialyte. *Lithos* 294–295, 73–86. https://doi.org/10.1016/j.lithos.2017.09.023

Söderlund, U., Isachsen, C.E., Bylund, G., Heaman, L.M., Patchett, P.J., Vervoort, J.D., Andersson, U.B. (2005) U–Pb baddeleyite ages and Hf, Nd isotope chemistry constraining repeated mafic magmatism in the Fennoscandian Shield from 1.6 to 0.9 Ga. *Contributions to Mineralogy and Petrology* 150, 174–194. https://doi.org/10.1007/s00410-005-0011-1

Söderlund, U., Elming, S.-Å., Ernst, R.E., Schissel, D. (2006) The Central Scandinavian Dolerite Group—Protracted hotspot activity or back-arc magmatism?: Constraints from U–Pb baddeleyite geochronology and Hf isotopic data. *Precambrian Research* 150, 136–152. https://doi.org/10.1016/j.precamres.2006.07.004

Tichomirowa, M., Whitehouse, M.J., Gerdes, A., Götze, J., Schulz, B., Belyatsky, B.V. (2013) Different zircon recrystallization types in carbonatites caused by magma mixing: Evidence from U–Pb dating, trace element and isotope composition (Hf and O) of zircons from two Precambrian carbonatites from Fennoscandia. *Chemical Geology* 353, 173–198. https://doi.org/10.1016/j.chemgeo.2012.11.004

Vervoort, J.D., Patchett, P.J. (1996) Behavior of hafnium and neodymium isotopes in the crust: Constraints from Precambrian crustally derived granites. *Geochimica et Cosmochimica Acta* 60, 3717–3733. https://doi.org/10.1016/0016-7037(96)00201-3

Vetrin, V.R., Belousova, E.A. (2020) The Lu–Hf Isotope Composition of Zircon from Syenites of the Saharjok Alkaline Massif, Kola Peninsula. *Geology of Ore Deposits* 62, 574–583. https://doi.org/10.1134/S1075701520070132

Vetrin, V.R., Belousova, E.A., Kremenetsky, A.A. (2018) Lu–Hf Isotopic Systematics of Zircon From Lower Crustal Xenoliths in the Belomorian Mobile Belt. *Geology of Ore Deposits* 60, 568–577. https://doi.org/10.1134/S1075701518070085

Westhues, A., Hanchar, J.M., LeMessurier, M.J., Whitehouse, M.J. (2017) Evidence for hydrothermal alteration and source regions for the Kiruna iron oxide–apatite ore (northern Sweden) from zircon Hf and O isotopes. *Geology* 45, 571–574. https://doi.org/10.1130/G38894.1

References for Zircon Lu-Hf Isotope Data from SW Greenland

Amelin, Y., Kamo, S.L., Lee, D.-C. (2011) Evolution of early crust in chondritic or non-chondritic Earth inferred from U–Pb and Lu–Hf data for chemically abraded zircon from the Itsaq Gneiss Complex, West Greenland. *Canadian Journal of Earth Sciences* 48, 141–160. https://doi.org/10.1139/E10-091

Fisher, C.M., Vervoort, J.D. (2018) Using the magmatic record to constrain the growth of continental crust—The Eoarchean zircon Hf record of Greenland. *Earth and Planetary Science Letters* 488, 79–91. https://doi.org/10.1016/j.epsl.2018.01.031

Hiess, J., Bennett, V.C., Nutman, A.P., Williams, I.S. (2009) In situ U–Pb, O and Hf isotopic compositions of zircon and olivine from Eoarchaean rocks, West Greenland: New insights to making old crust. *Geochimica et Cosmochimica Acta* 73, 4489–4516. https://doi.org/10.1016/j.gca.2009.04.019

Hiess, J., Bennett, V.C., Nutman, A.P., Williams, I.S. (2011) Archaean fluid-assisted crustal cannibalism recorded by low $\delta^{18}O$ and negative $\varepsilon_{Hf(T)}$ isotopic signatures of West Greenland granite zircon. *Contributions to Mineralogy and Petrology* 161, 1027–1050. https://doi.org/10.1007/s00410-010-0578-z

Kemp, A.I.S., Foster, G.L., Scherstén, A., Whitehouse, M.J., Darling, J., Storey, C. (2009) Concurrent Pb–Hf isotope analysis of zircon by laser ablation multi-collector ICP-MS, with implications for the crustal evolution of Greenland and the Himalayas. *Chemical Geology* 261, 244–260. https://doi.org/10.1016/j.chemgeo.2008.06.019

Kemp, A.I.S., Whitehouse, M.J., Vervoort, J.D. (2019) Deciphering the zircon Hf isotope systematics of Eoarchean gneisses from Greenland: Implications for ancient crust-mantle differentiation and Pb isotope controversies. *Geochimica et Cosmochimica Acta* 250, 76–97. https://doi.org/10.1016/j.gca.2019.01.041

Næraa, T., Scherstén, A., Rosing, M.T., Kemp, A.I.S., Hoffmann, J.E., Kokfelt, T.F., Whitehouse, M.J. (2012) Hafnium isotope evidence for a transition in the dynamics of continental growth 3.2 Gyr ago. *Nature* 485, 627–630. https://doi.org/10.1038/nature11140

Næraa, T., Kemp, A.I.S., Scherstén, A., Rehnström, E.F., Rosing, M.T., Whitehouse, M.J. (2014) A lower crustal mafic source for the ca. 2550 Ma Qôrqut Granite Complex in southern West Greenland. *Lithos* 192–195, 291–304. https://doi.org/10.1016/j.lithos.2014.02.013

Næraa, T., Kokfelt, T.F., Scherstén, A., Petersson, A. (2018) The ca. 2785–2805 Ma High Temperature Ilivertalik Intrusive Complex of Southern West Greenland. *Geosciences* 8, 319. https://doi.org/10.3390/geosciences8090319

References for Zircon Lu-Hf Isotope Data from Pilbara

Amelin, Y., Lee, D.-C., Halliday, A.N. (2000) Early-middle Archaean crustal evolution deduced from Lu-Hf and U-Pb isotopic studies of single zircon grains. *Geochimica et Cosmochimica Acta* 64, 4205–4225. https://doi.org/10.1016/S0016-7037(00)00493-2

Gardiner, N.J., Hickman, A.H., Kirkland, C.L., Lu, Y., Johnson, T., Zhao, J.-X. (2017) Processes of crust formation in the early Earth imaged through Hf isotopes from the East Pilbara Terrane. *Precambrian Research* 297, 56–76. https://doi.org/10.1016/j.precamres.2017.05.004

Guitreau, M., Blichert-Toft, J., Martin, H., Mojzsis, S.J., Albarède, F. (2012) Hafnium isotope evidence from Archean granitic rocks for deep-mantle origin of continental crust. *Earth and Planetary Science Letters* 337–338, 211–223. https://doi.org/10.1016/j.epsl.2012.05.029

Kemp, A.I.S., Hickman, A.H., Kirkland, C.L., Vervoort, J.D. (2015) Hf isotopes in detrital and inherited zircons of the Pilbara Craton provide no evidence for Hadean continents. *Precambrian Research* 261, 112–126. https://doi.org/10.1016/j.precamres.2015.02.011

Kemp, A.I.S., Vervoort, J.D., Petersson, A., Smithies, R.H., Lu, Y. (2023) A linked evolution for granite-greenstone terranes of the Pilbara Craton from Nd and Hf isotopes, with implications for Archean continental growth. *Earth and Planetary Science Letters* 601, 117895. https://doi.org/10.1016/j.epsl.2022.117895

Petersson, A., Kemp, A.I.S., Hickman, A.H., Whitehouse, M.J., Martin, L., Gray, C.M. (2019a) A new 3.59 Ga magmatic suite and a chondritic source to the east Pilbara Craton. *Chemical Geology* 511, 51–70. https://doi.org/10.1016/j.chemgeo.2019.01.021

Petersson, A., Kemp, A.I.S., Whitehouse, M.J. (2019b) A Yilgarn seed to the Pilbara Craton (Australia)? Evidence from inherited zircons. *Geology* 47, 1098–1102. https://doi.org/10.1130/G46696.1

Petersson, A., Kemp, A.I.S., Gray, C.M., Whitehouse, M.J. (2020) Formation of early Archean Granite-Greenstone Terranes from a globally chondritic mantle: Insights from igneous rocks of the Pilbara Craton, Western Australia. *Chemical Geology* 551, 119757. https://doi.org/10.1016/j.chemgeo.2020.119757